Electronic Supplementary Material (ESI) for ChemComm.

SUPPORTING INFORMATION

Double Intramolecular Hydrogen Transfer Assisted Dual Emission in Carbazole-embedded Porphyrin-like Macrocycle

1. General Information:

The reagents and materials for the synthesis were used as obtained from Sigma-Aldrich chemical suppliers. All solvents were purified and dried by standard methods prior to use. Silica gel column chromatography was performed on Wakogel C-200 and C-300. Alumina column chromatography was performed on Active alumina (basic). Thin-layer chromatography (TLC) was carried out on aluminum sheets coated with silica gel 60 F254 (Merck 5554). Recrystallized samples of porphyrinoids were utilized for all the spectroscopic measurements. ^{1}H NMR (500 MHz) and ^{13}C NMR (125 MHz) spectra were recorded on INOVA 500 (Varian) spectrometer, and chemical shifts were reported as the delta scale in ppm relative to $CHCl_3$ as an internal reference for ^{1}H (δ = 7.26 ppm) and for ^{13}C (δ =77.0 ppm). High-resolution mass spectra (HRMS) were recorded on Q-exactive Orbitrap mass spectrometer based on the electrospray ionization method.

Cyclic and differential-pulse voltammetric measurements were performed on a PC-controlled electrochemical analyzer (CH instruments model CHI620C) using a conventional three-electrode cell for samples (1 mM) dissolved in dry CH_3CN containing 0.1 M *n*-Bu_4NPF_6 ($TBAPF_6$) as the supporting electrolyte. Measurements were carried out under an Argon atmosphere. A Glassy carbon working electrode, a calomel reference electrode and platinum wire counter electrode were used in all electrochemical experiments. The potentials were calibrated using the ferrocenium/ferrocene couple. The optical absorption spectra were recorded on a Shimadzu (Model UV-3600) spectrophotometer. Concentrations of solutions are *ca.* to be 1 x 10^{-6} M (porphyrin Soret band) and 5 x 10^{-5} M (porphyrin Q-bands).

X-ray Crystal Structure Analysis:
Single crystal X-ray intensity data were collected on a Bruker KAPPA APEXII diffractometer in omega and phi scan mode, MoKα = 0.71073 Å at 298 K.

Computational Details: All calculations were carried out using the Gaussian 16 program.[S1] Initial geometries were obtained from X-ray structures. Calculations were performed using the density functional theory (DFT) method at B3LYP (Becke's three-parameter hybrid exchange

functionals and the Lee-Yang-Parr correlation functional) level, employing a 6-31G(d) basis set. Vertical electronic excitations based on B3LYP optimized geometries were computed using the time-dependent density functional theory (TDDFT) formalism at the same level of theory. NICS (0) values were calculated using NMR keyword with GIAO method. Further, we have performed NICS XY-scan for a grid of 0.5 Å along x and y-axes by placing the ghost atoms (Bq) at a distance of 0.1 Å to generate a grid of 11x11 points. Next, we have plotted AICD plots to observe the ring current using NMR keyword with CSGT method.[S2]

2. Synthetic Procedures and Compound Data:

Precursors:

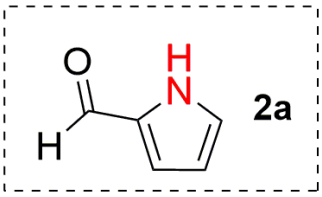

Commercially available **2a** was recrystallized using $CHCl_3$/ *n*-hexane and subjected to ^1H and ^{13}C NMR characterization. ^1H NMR (500 MHz, $CDCl_3$, 298 K) δ = 10.58 (br s, 1H, NH), 9.49 (d, J = 0.7 Hz, 1H), 7.17 (s, 1H), 7.00 (t, J = 2.6 Hz, 1H), 6.34 (t, J = 3.6 Hz, 1H); ^{13}C NMR (125 MHz, $CDCl_3$) δ = 179.5, 132.8, 127.1, 122.0, 111.3.

pyrrole-2,5-dicarboxaldehyde (2b):

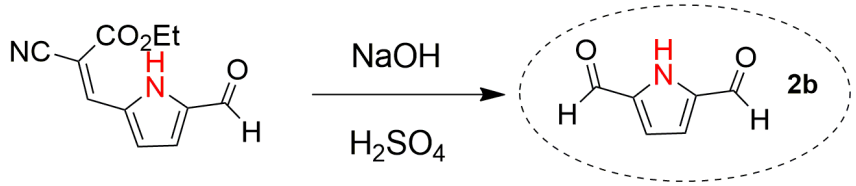

40%

By slightly modified literature method,[S3] the aldehyde is deprotected *via* alkaline hydrolysis, Ethyl α-cyano-5-formyl-2-pyrroleacrylate (1 g, 4.58 mmol) was added to a 4 M aqueous solution of sodium hydroxide (15 mL) and refluxed for 3 h. The mixture was then cooled below 20 °C and acidified with conc. sulfuric acid before passing through a filter, removing a black powdery byproduct. The product was extracted with ethyl acetate. The combined organic extract was washed with water, dried over anhydrous Na_2SO_4 and concentrated in vacuo. This crude material was further purified by flash

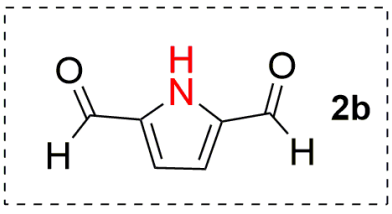

column chromatography [silica; ethyl acetate/CH_2Cl_2 (1:9)] afforded pure **2b** as a white powder (0.23 g, 40% yield). ^{1}H NMR (500 MHz, $CDCl_3$, 298 K) δ = 10.71 (br s, 1H, NH), 9.78 (s, 2H), 7.01 (d, J = 2.2 Hz, 2H); ^{13}C NMR (125 MHz, $CDCl_3$) δ = 181.6, 135.8, 119.5; HRMS (ESI) m/z: $[M-H]^-$ Calcd for $C_6H_4NO_2$ 122.0242; Found 122.0235; mp = 180 °C.

(perfluorophenyl)(1*H*-pyrrol-2-yl)methanol (6a):

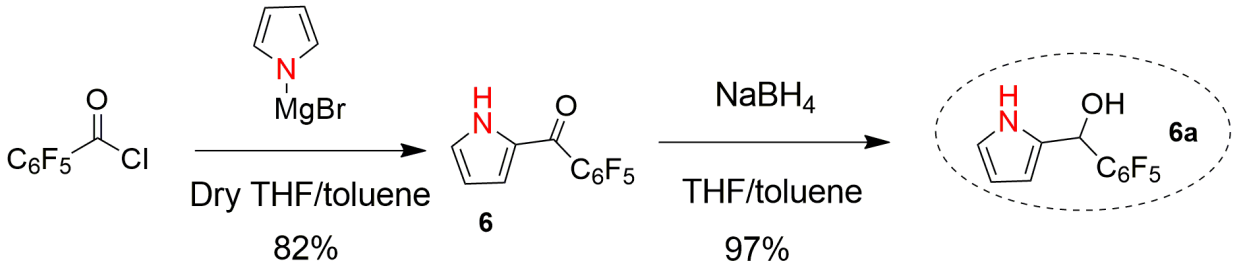

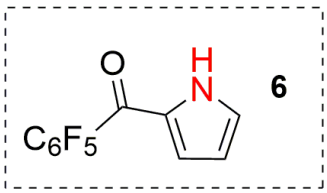

Compound **6** was synthesized according to the reported method.[S4] Pyrrolyl-N-magnesium bromide (3.0 equiv., 43.2 mmol, prepared from PhMgBr in THF (2.0 M, 3.2 equiv., 46.0 mmol) diluted with anhydrous toluene (5 mL) and pyrrole (1.04 mL, 14.4 mmol)) was added dropwise to a solution of pentafluorobenzoyl chloride (0.692 mL, 47.0 mmol) in anhydrous THF (10 mL)at 0 °C under Argon. After the resulting solution was stirred for 30 min at 0 °C and another 30 min at room temperature, the reaction mixture was quenched by addition of a saturated aqueous NH_4Cl (5 mL). The product was extracted with ethyl acetate. The combined organic extract was washed with water, dried over anhydrous Na_2SO_4 and concentrated in vacuo. The mixture was subjected to flash column chromatography [silica; CH_2Cl_2/ petroleum ether (3:7)] afforded pure **6** as a white powder (1.02 g, 82% yield). ^{1}H NMR (500 MHz, $CDCl_3$, 298 K) δ = 9.90 (br s, 1H, NH), 7.24 (s, 1H), 6.72 (s, 1H), 6.36 (m, 1H); ^{13}C NMR (125 MHz, $CDCl_3$) δ = 172.5, 131.5, 128.3, 121.6, 112.1; HRMS (ESI) m/z: $[M+H]^+$ Calcd for $C_{11}H_5F_5NO$ 262.0291; Found 262.0283; mp = 165 °C.

Reduction of 6: A solution of monoacylated dipyrromethane **6** (300 mg, 1.14 mmol) in dry THF/methanol (12 mL, 5:1) was treated with $NaBH_4$ (217 mg, 5.747 mmol) at 25 °C for 2 h. The reaction mixture was quenched with saturated aq. NH_4Cl (30 mL) and extracted with CH_2Cl_2. The organic phase was dried over Na_2SO_4 and

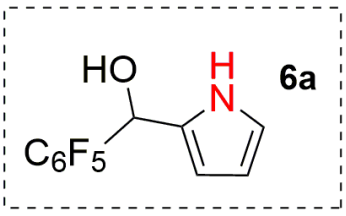

concentrated in vacuo to afford **6a**[S7] as a colorless solid (295 mg, 97%). ^{1}H NMR (500 MHz, $CDCl_3$) δ = 8.66 (br s, 1H, NH), 6.82 (d, J = 1.3 Hz, 1H), 6.22 (s, 1H), 6.14 (d, J = 3.0 Hz, 1H), 5.96 (s, 1H), 2.91 (br s, 1H, OH); ^{13}C NMR (125 MHz, $CDCl_3$) δ = 129.9, 119.0, 108.6, 106.9, 62.3; mp = 130 °C

1-(Pentafluorobenzoyl)-5-(pentafluorophenyl)dipyrromethane (7a):

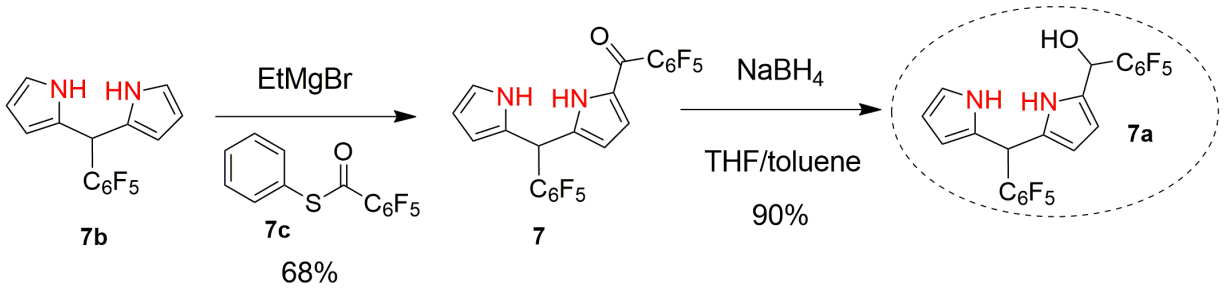

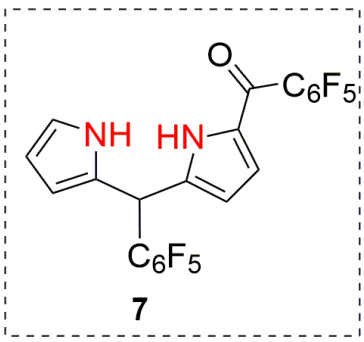

A slightly modified literature method,[S5] a solution of EtMgBr (8.0 mL, 8.0 mmol, 1.0 M in THF) was added slowly to a tap water cooled flask containing a solution of 5-(Pentafluorophenyl)dipyrromethane **(7b)** (1.0 g, 3.2 mmol) in THF (10 mL) under Ar. The mixture was stirred at room temperature for 10 min and then cooled to -78 °C. A solution of (pentafluorobenzoyl)pyridyl thioester **(7c)** (0.98 g, 32 mmol) in THF (10 mL) was then added over 10 min. The solution was maintained at -78 °C for 10 min, and then the cooling bath was removed. TLC [silica; CH_2Cl_2/*n*-hexane (3:2)] showed complete consumption of the pyridyl thioester after 15 min, so the reaction was quenched with saturated aqueous NH_4Cl. The mixture was allowed to warm to room temperature, poured into CH_2Cl_2, washed with water, and then dried (Na_2SO_4) and the solvent removed to afford a dark foam. Purification by flash column chromatography [silica; CH_2Cl_2/*n*-hexane (3:2)] afforded a pale brown solid **7** (1.10 g, 68%). Analytical data were identical to those previously reported.[S5] ^{1}H NMR (500 MHz, $CDCl_3$, 298 K) δ/ppm: 9.40 (br s, 1H, NH), 8.26 (br s, 1H, NH), 6.83-6.81 (m, 1H), 6.64 (s, 1H), 6.22-6.20 (m, 2H), 6.08 (t, J = 6.25 Hz, 1H), 5.92 (s, 1H). ^{13}C NMR (125 MHz, $CDCl_3$) δ = 172.1, 140.6, 131.2, 125.6, 122.4, 119.1, 111.2, 109.0, 109.0; HRMS (ESI) m/z: $[M-H]^-$ Calcd for $C_{22}H_7F_{10}N_2O$ 505.0398; Found 505.0405; mp = 160 °C.

Reduction of 7: A sample of mono acyl dipyrromethane **7** (0.1g, 0.19 mmol) was dissolved in Dry THF/Methanol (11mL, 10:1) at room temperature stirred in 25 mL two neck round bottom flask fitted with a vented rubber septum and flouted with argon. The septum was removed as needed to add $NaBH_4$ (0.15 g, 3.9 mmol). The progress of the reduction was monitored by TLC analysis [CH_2Cl_2]. After the reaction was complete, the reaction mixture was poured into a mixture of saturated aqueous NH_4Cl (10 mL). The organic phase was extracted by CH_2Cl_2 and dried over Na_2SO_4 and the solvent was removed under vacuum afforded DPM mono carbinol **7a** in 90%.^{1}H NMR (500 MHz, $CDCl_3$, 298 K) δ/ppm: 8.65 (d, J = 28.2 Hz, 1H, NH) 8.34 (br s, 1H, NH), 6.70 (s, 1H), 6.18 (s, 1H), 6.11 (s, 1H), 6.06 (d, J = 15.25 Hz, 1H), 5.87 (s, 2H), 5.79 (s, 1H), 2.89 (br s, 1H, OH). ^{13}C NMR (125 MHz, $CDCl_3$) δ = 130.1, 129.7, 127.9, 127.7, 118.4, 108.6, 107.9, 107.7, 107.7, 107.0, 62.0; HRMS (ESI) m/z: $[M-H]^-$ Calcd for $C_{22}H_9F_{10}N_2O$ 507.0555; Found 507.0566; mp = 115 °C

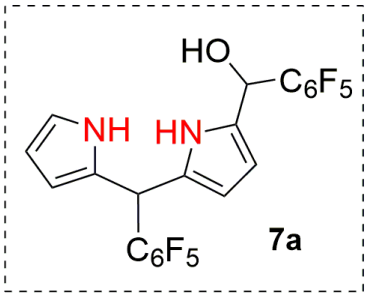

Route A:

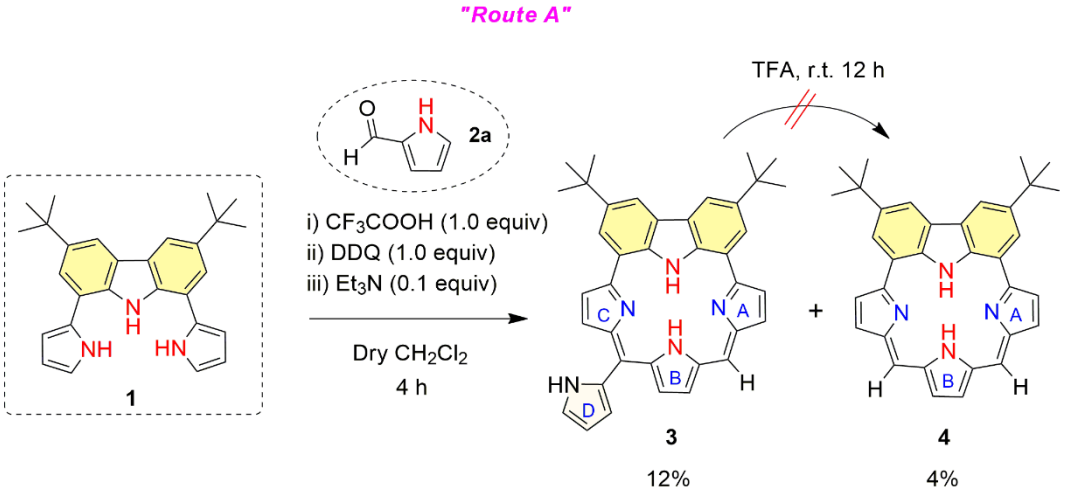

To a solution of 1,8-Di(-1*H*-pyrrole)-3,6- di-*tert*-butyl)-9*H* carbazole **1** (100 mg, 0.244 mmol) and 1*H*-pyrrole-2-carboxaldehyde **2a** (23.2 mg, 0.244 mmol) was dissolved in 50 mL of dry CH_2Cl_2. To this, CF_3COOH (27.9 µL, 0.244 mmol) was added under argon and the solution was stirred for 4 h at room temperature under dark. Then, the reaction was quenched with few drops of trimethylamine followed by the drop wise addition of DDQ (55.4 mg, 0.244 mmol) in 10 mL

CH_2Cl_2. The crude reaction mixture was passed through a short pad of basic alumina and the green fraction was collected and concentrated under vacuum. Further purification was done by silica gel column (240-400 mesh) chromatography.

Macrocycle 3 was isolated and precipitated using *n*-hexane to afford pure **3** in 12% yield. ^{1}H NMR (500 MHz, $CDCl_3$, 298 K) δ = 8.78 (br s, 1H, NH), 8.78 (s, 2H), 8.74 (s, 1H), 8.70 (br s, 1H, NH), 8.68 (s, 1H), 8.62 (br s, 1H, NH), 8.07-8.05 (m, 2H), 7.78 (d, J = 4.5 Hz, 2H), 7.72 (d, J = 4.5 Hz, 2H), 7.64 (s, 1H), 7.30 (s, 1H), 7.28 (s, 1H), 7.04 (s, 1H), 6.72 (s, 1H), 6.47 (d, J = 3.0 Hz, 1H), 1.70 (s, 9H), 1.69 (s, 9H); ^{13}C NMR (125 MHz, $CDCl_3$) δ = 168.1, 167.0, 152.2, 142.2, 138.0, 137.1, 136.3, 136.1, 135.4, 129.2, 124.8, 124.7, 124.6, 124.5, 124.4, 124.3, 123.9, 123.0, 122.5, 119.8, 119.6, 118.7, 115.1, 114.5, 109.4, 35.2, 32.3; UV/Vis/NIR (CH_2Cl_2): λ_{max}/nm (ε [mol^{-1} dm^3 cm^{-1}]): 292 (11017), 329 (13058), 422 (17583), 580 (8643), 626 (9719). HRMS (ESI) m/z: $[M+H]^+$ Calcd for $C_{38}H_{36}N_5$ 562.2971; Found 562.2961; mp = 95 °C

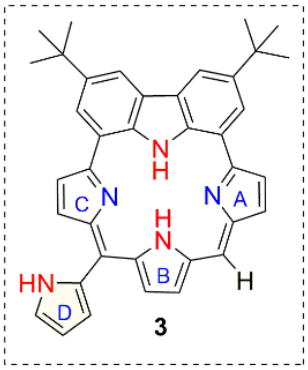

3

Macrocycle 4 was isolated and precipitated using *n*-hexane to afford pure **4** in 4% yield. ^{1}H NMR (500 MHz, $CDCl_3$, 298 K) δ = 8.77 (s, 2H), 8.64 (s, 2H), 8.16 (br s, 1H, NH), 7.98 (br s, 1H, NH), 7.97 (d, J = 4.0 Hz, 2H), 7.64 (d, J = 4.5 Hz, 2H), 7.44 (s, 2H), 7.19 (s, 2H), 1.72 (s, 18H); ^{13}C NMR (125 MHz, $CDCl_3$) δ = 167.5, 152.3, 141.8, 136.6, 136.1, 135.7, 124.6, 124.4, 124.2, 122.0, 119.6, 117.7, 113.9, 35.1, 32.4; UV/Vis/NIR (CH_2Cl_2): λ_{max}/nm (ε [mol^{-1} dm^3 cm^{-1}]): 291 (42387), 329 (69822), 375 (81290), 572 (35274), 621 (50080). HRMS (ESI) m/z: $[M+H]^+$ Calcd for $C_{34}H_{33}N_4$ 497.2705; Found 497.2709; mp = 120 °C

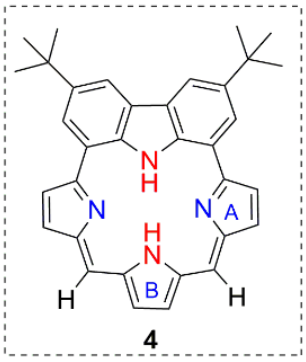

4

Macrocycle 4 from **Route B**:

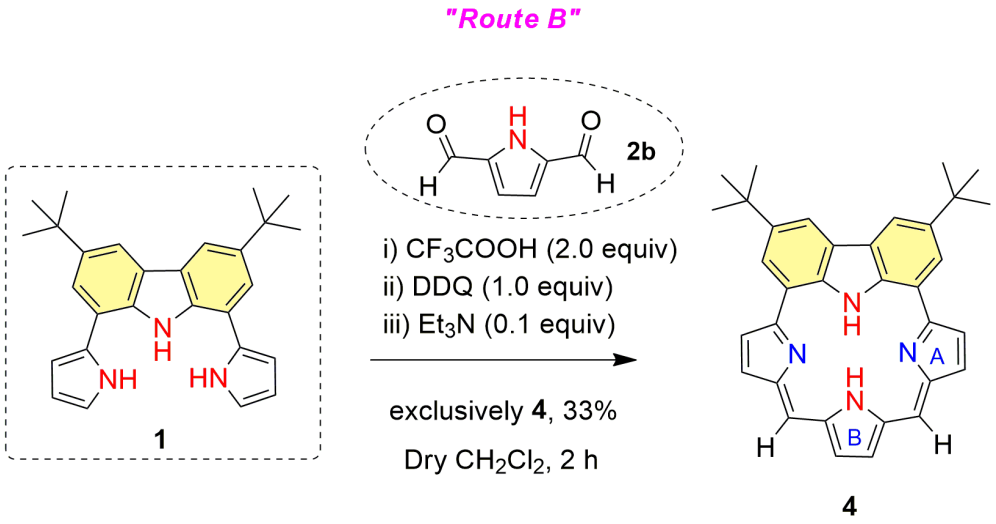

To a solution of **1** (100 mg, 0.244 mmol) and 1*H*-pyrrole-2,5-dicarboxaldehyde **2b** (30 mg, 0.244 mmol) was dissolved in 50 mL of dry CH_2Cl_2. To this, CF_3COOH (55.8 µL, 0.488 mmol) was added under argon and the solution was stirred for 2 h at room temperature under dark. Then, the reaction was quenched with few drops of trimethylamine followed by the drop wise addition of DDQ (55.4 mg, 0.244 mmol) in 10 mL CH_2Cl_2. The crude reaction mixture was passed through a short pad of basic alumina and the green fraction was collected and concentrated under vacuum. Further purification was done by silica gel column (240-400 mesh) chromatography. The green colored fraction was isolated and precipitated using *n*-hexane to afford pure **4** in 33% (40 mg) yield.

Macrocycle 5 from **Route C:**

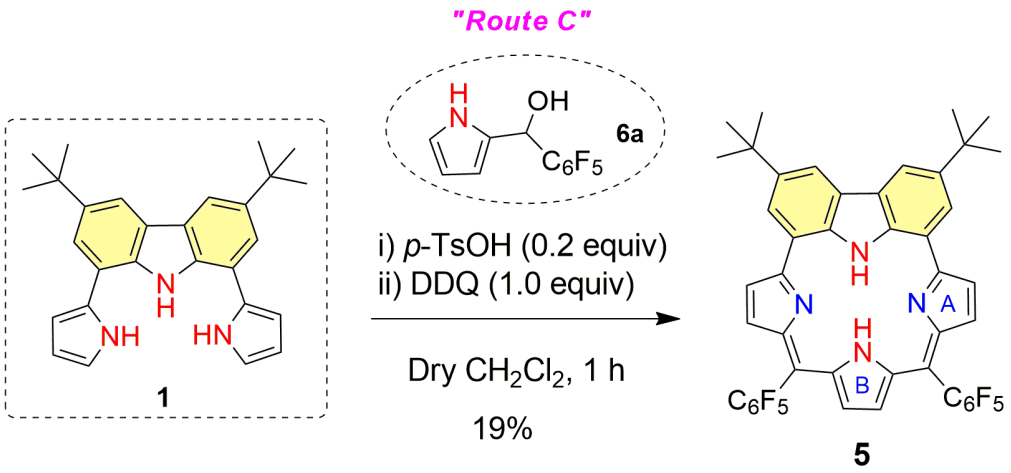

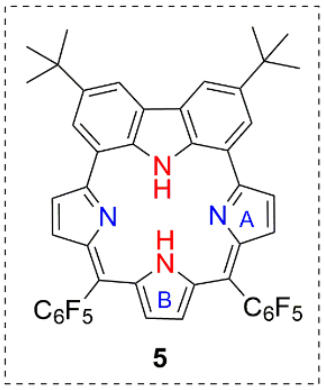

5

To a 250 mL round bottom flask containing compound **1** (0.1 g, 0.244 mmol) and (perfluorophenyl)(1*H*-pyrrol-2-yl)methanol **6a** (0.064 g, 0.244 mmol) was added in 100 ml of dry CH_2Cl_2 and stirred for 1 h under Ar atmosphere under dark. *Para*-toluenesulfonic acid (*p*-TsOH) (0.01 g, 0.0488 mmol) was added and the mixture was allowed to stir for 1 h. To the reaction mixture, 2,3-dichloro-5,6-dicyano-*p*-benzoquinone (DDQ) (0.056 g, 0.244 mmol) was added and allowed to stir for further 10 min at room temperature. The entire reaction mixture was filtered through a pad of basic alumina and eluted with CH_2Cl_2 until the eluent was no longer dark. The resulting crude mixture was concentrated by rotary evaporator to give a dark solid. The crude solid was purified by basic alumina column followed by silica-gel chromatography (240-400 mesh). The violet fraction eluted with 10% CH_2Cl_2/*n*-hexane provided **5** as dark green solid in 19% (40 mg) yield. ^{1}H NMR (500 MHz, $CDCl_3$, 298 K): δ = 8.94 (d, *J* = 1.0 Hz, 2H), 8.84 (s, 2H), 8.41 (br s, 1H, NH), 8.35 (br s, 1H, NH), 8.26 (d, *J* = 5.0 Hz, 2H), 7.47 (d, *J* = 4.5Hz, 2H), 6.95 (s, 2H), 1.71 (s, 18H); ^{13}C NMR (125 MHz, $CDCl_3$) *δ* = 169.3, 153.3, 142.9, 136.3, 136.1, 134.9, 127.3, 125.0, 124.6, 121.5, 121.1, 114.5, 113.6, 35.3, 32.3; UV/Vis/NIR (CH_2Cl_2): λ_{max}/nm (ε [mol^{-1} dm^3 cm^{-1}]): 291 (34106), 339 (46483), 385 (55887), 582 (24438), 632 (33438). HRMS (ESI) m/z: $[M+H]^+$ Calcd for $C_{46}H_{31}F_{10}N_4$ 829.2389; Found 829.2374; mp = 135 °C

Macrocycle 5 from **Route D:**

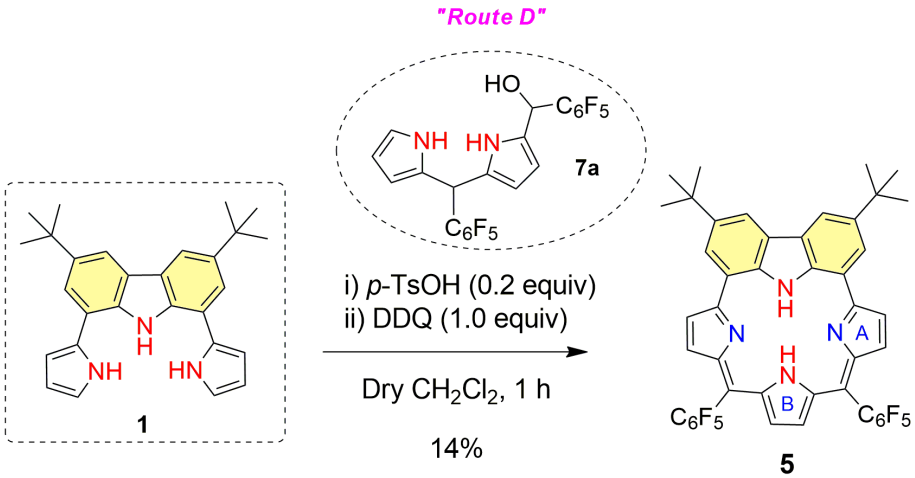

5

The above procedure was followed by using **1** (0.100 g, 0.244 mmol), and DPM mono carbinol **7a**[S8] (0.124 g, 0.244 mmol), *p*-TsOH (0.01 g, 0.0488 mmol) and DDQ (0.056 g, 2.88 mmol).

The green fraction was eluted with 5% *n*-hexane afforded **5** as dark green solid in 14% (29 mg) yield. Analytical data were identical to above method (**Route D**)

Plausible Mechanisms for the formation of macrocycles 3-5 is shown below:

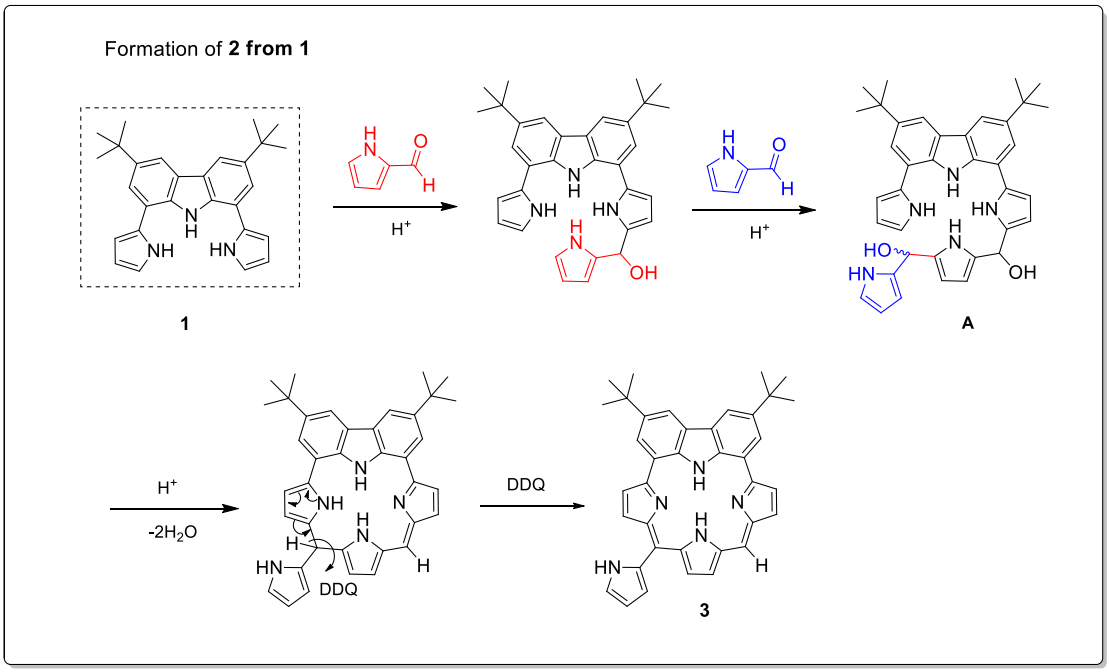

Formation of 3 from 1 and 5

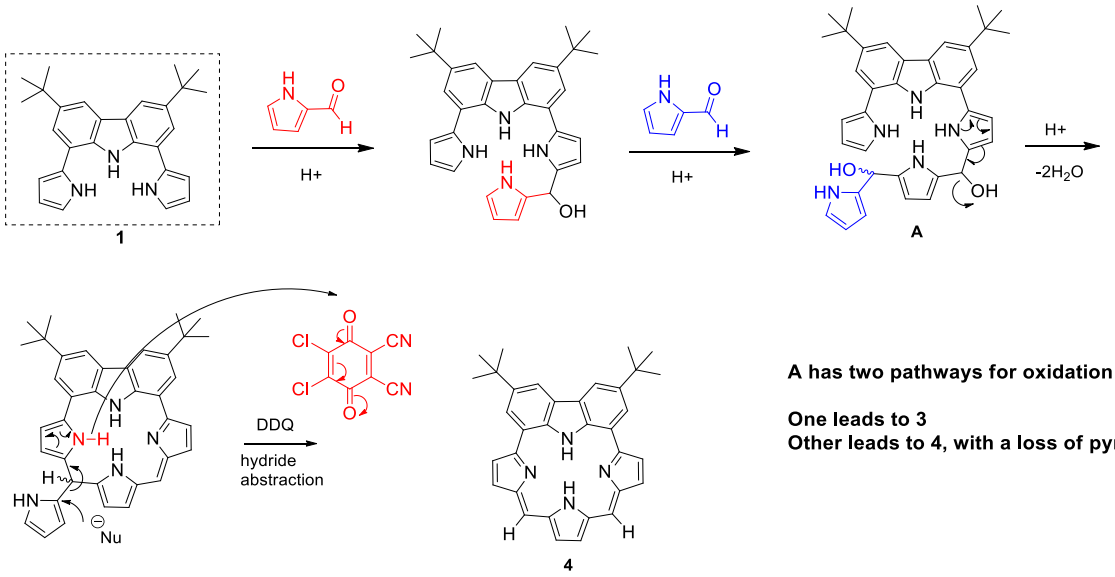

A has two pathways for oxidation

One leads to 3
Other leads to 4, with a loss of pyrrole nucleus

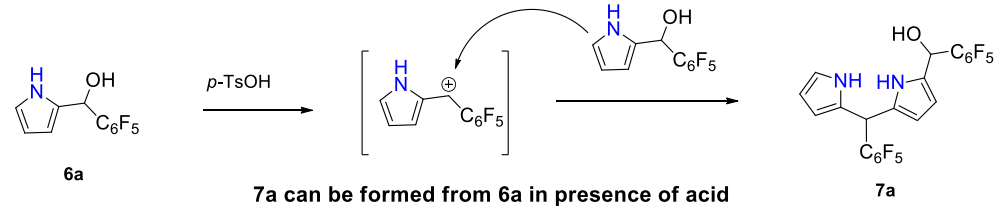

7a can be formed from 6a in presence of acid
Probably this is faster than reaction of 5 with 1
Therefore, 7a will react further with 1 as shown below

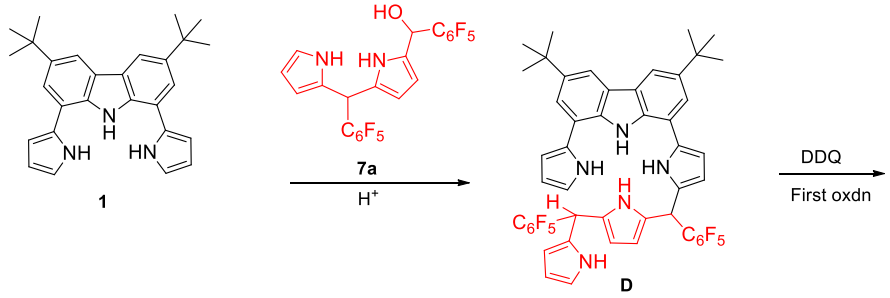

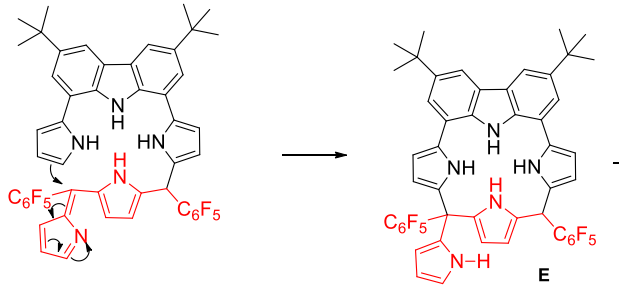

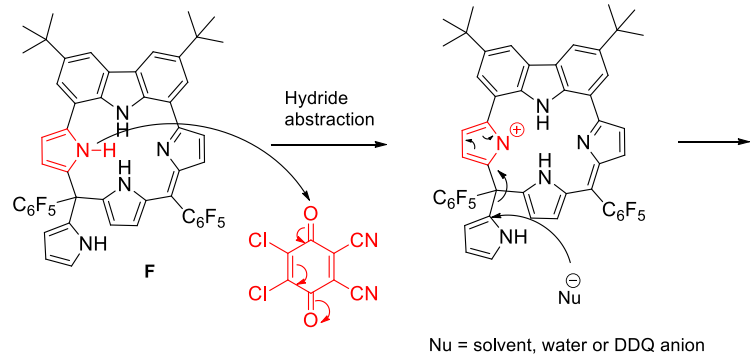

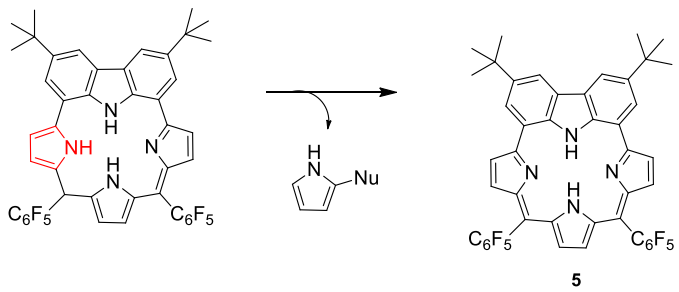

The hydride loss in third oxidation may happen from any of the four NHs in **F**
Subsequent proton loss and double bond shifts will complete the oxidation

3. High-Resolution MS

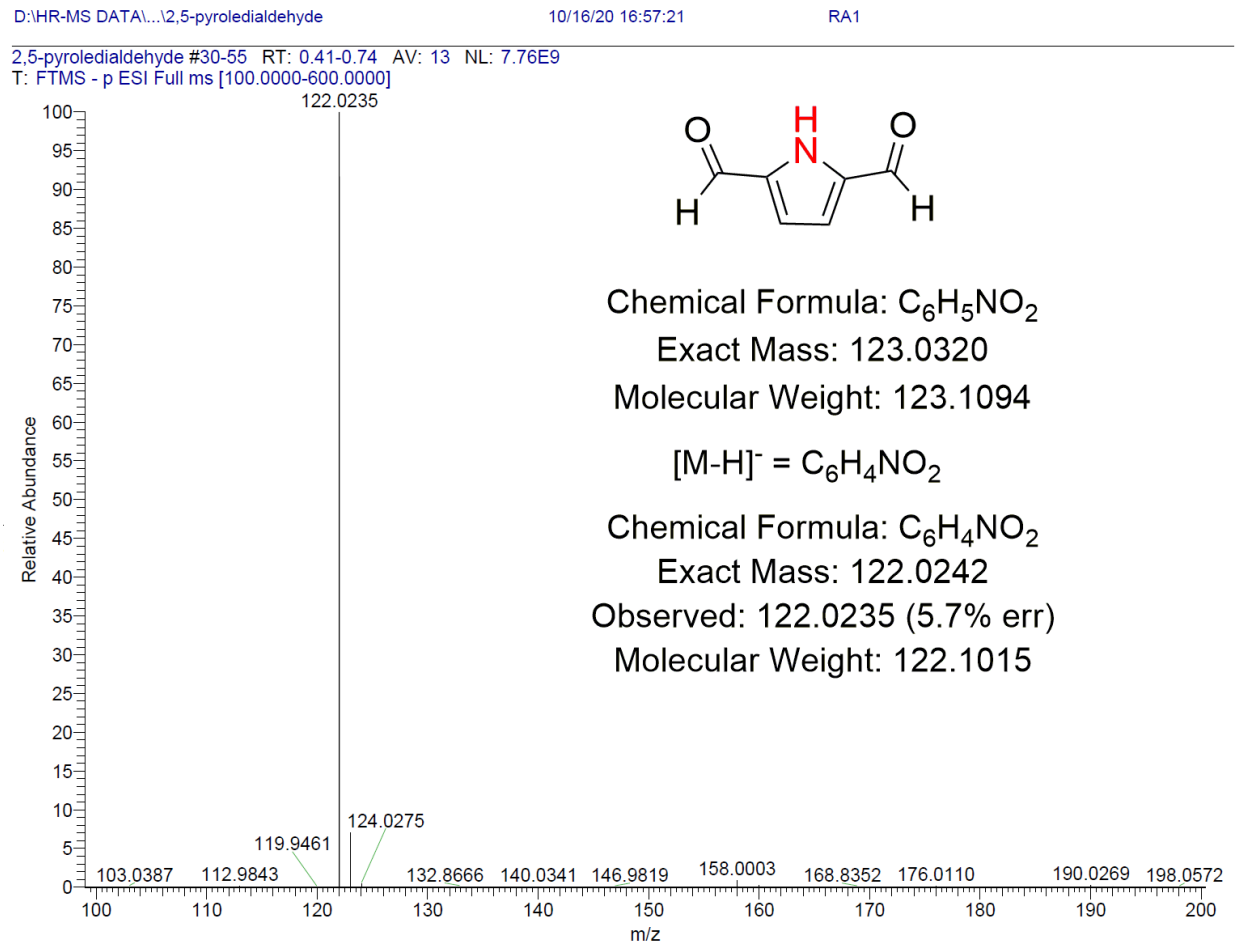

Figure S3.1. HR-MS (ESI) spectrum of **2b**.

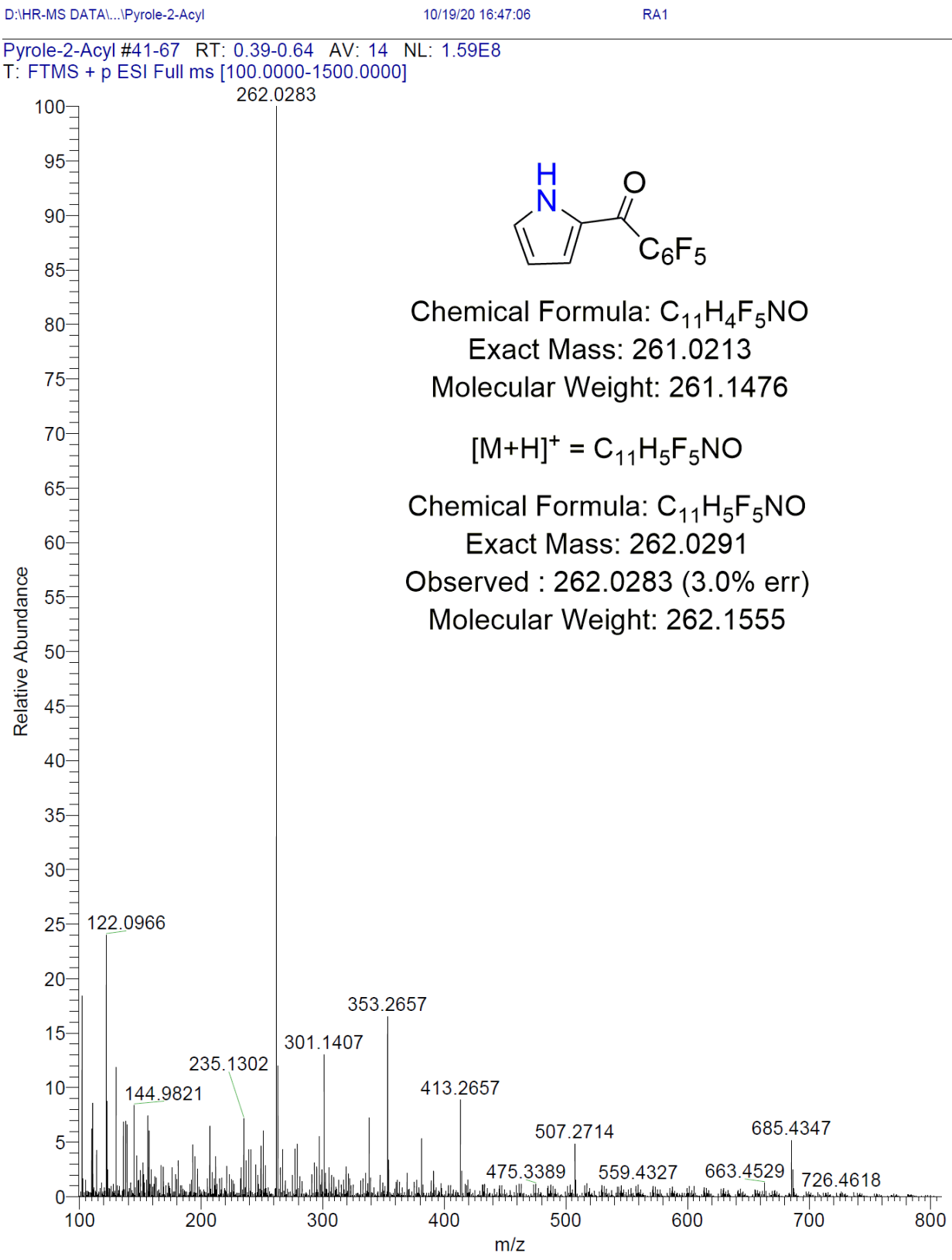

Figure S3.2. HR-MS (ESI) spectrum of **6**.

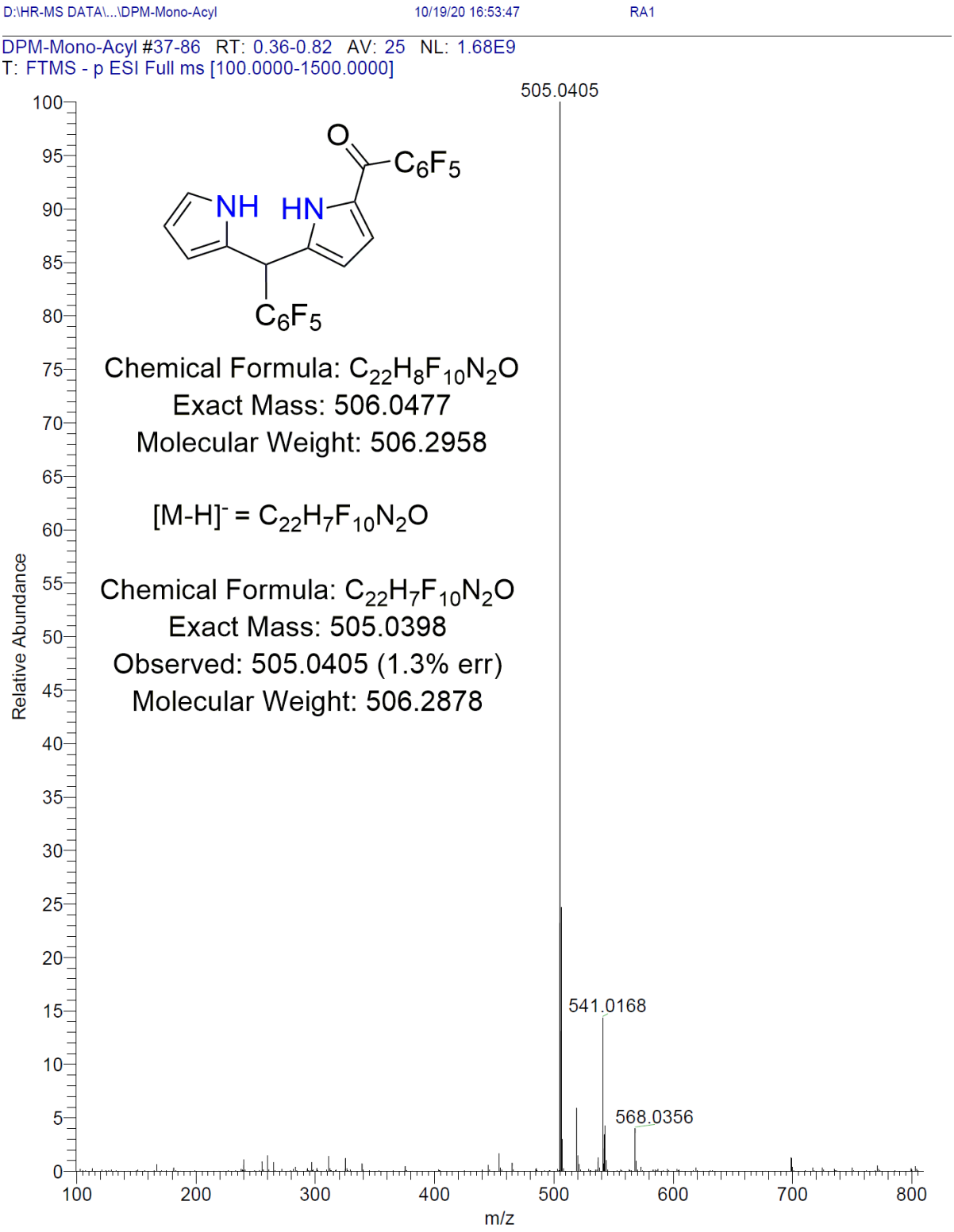

Figure S3.3. HR-MS (ESI) spectrum of **7**.

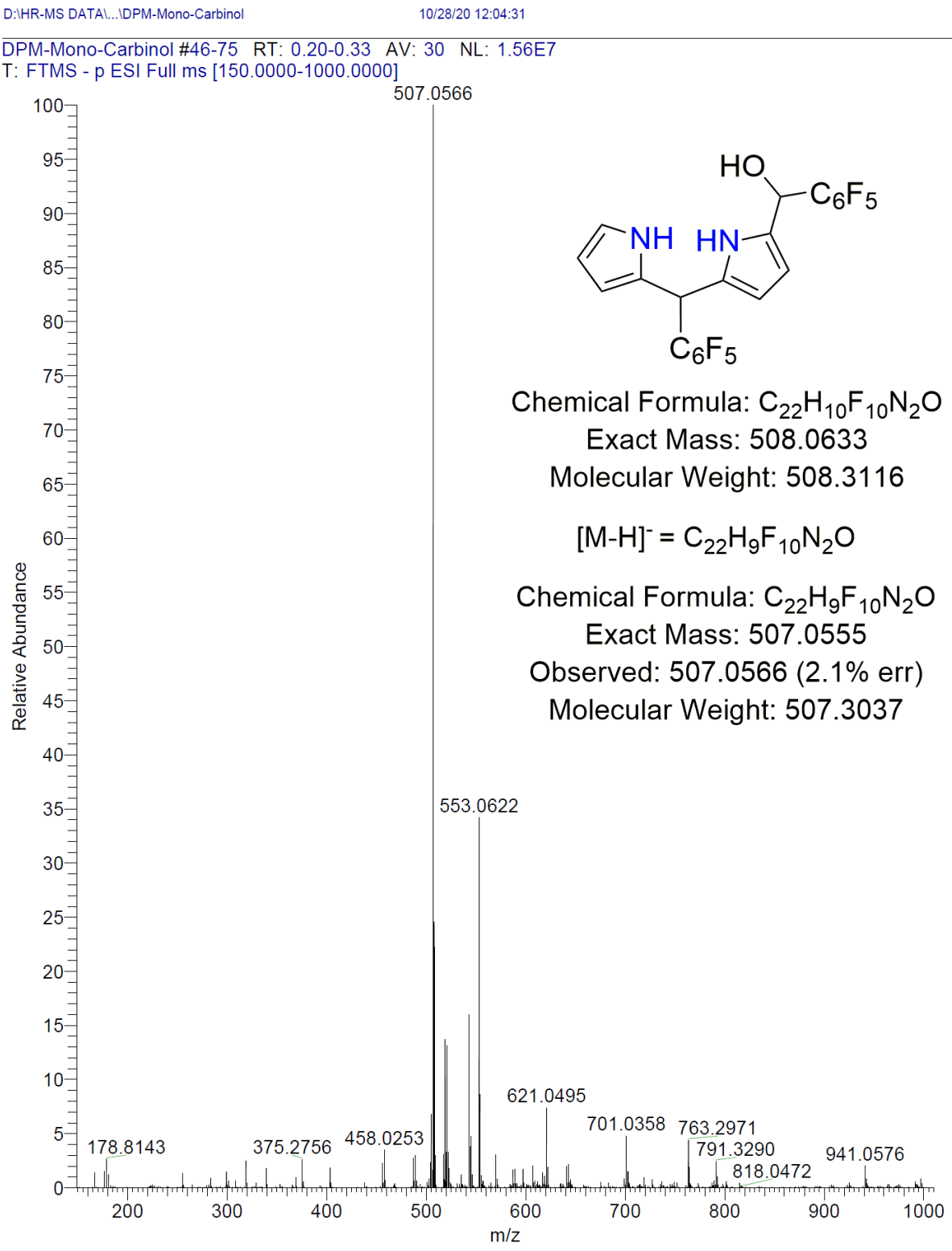

Figure S3.4. HR-MS (ESI) spectrum of **7a**.

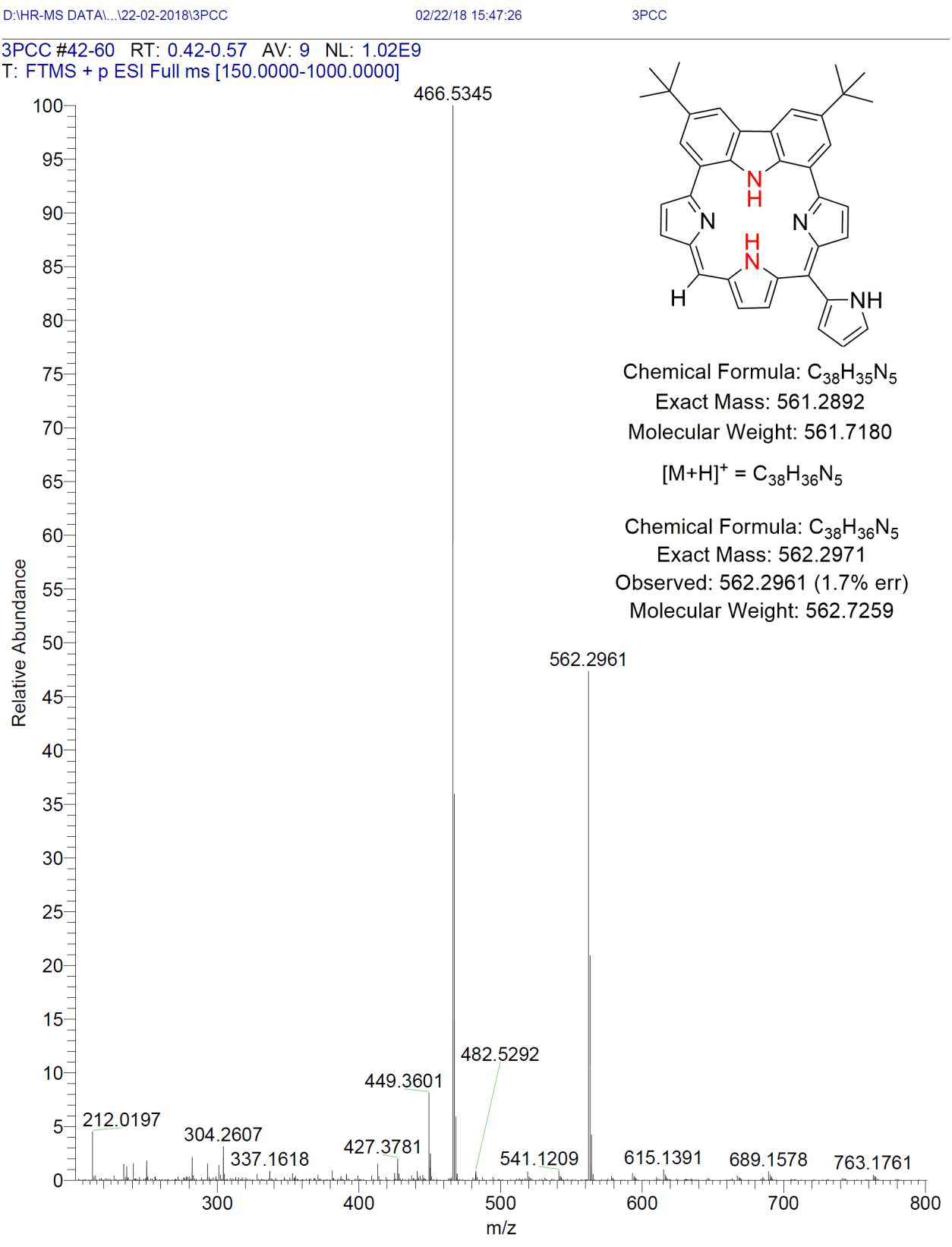

Figure S3.5. HR-MS (ESI) spectrum of **3**.

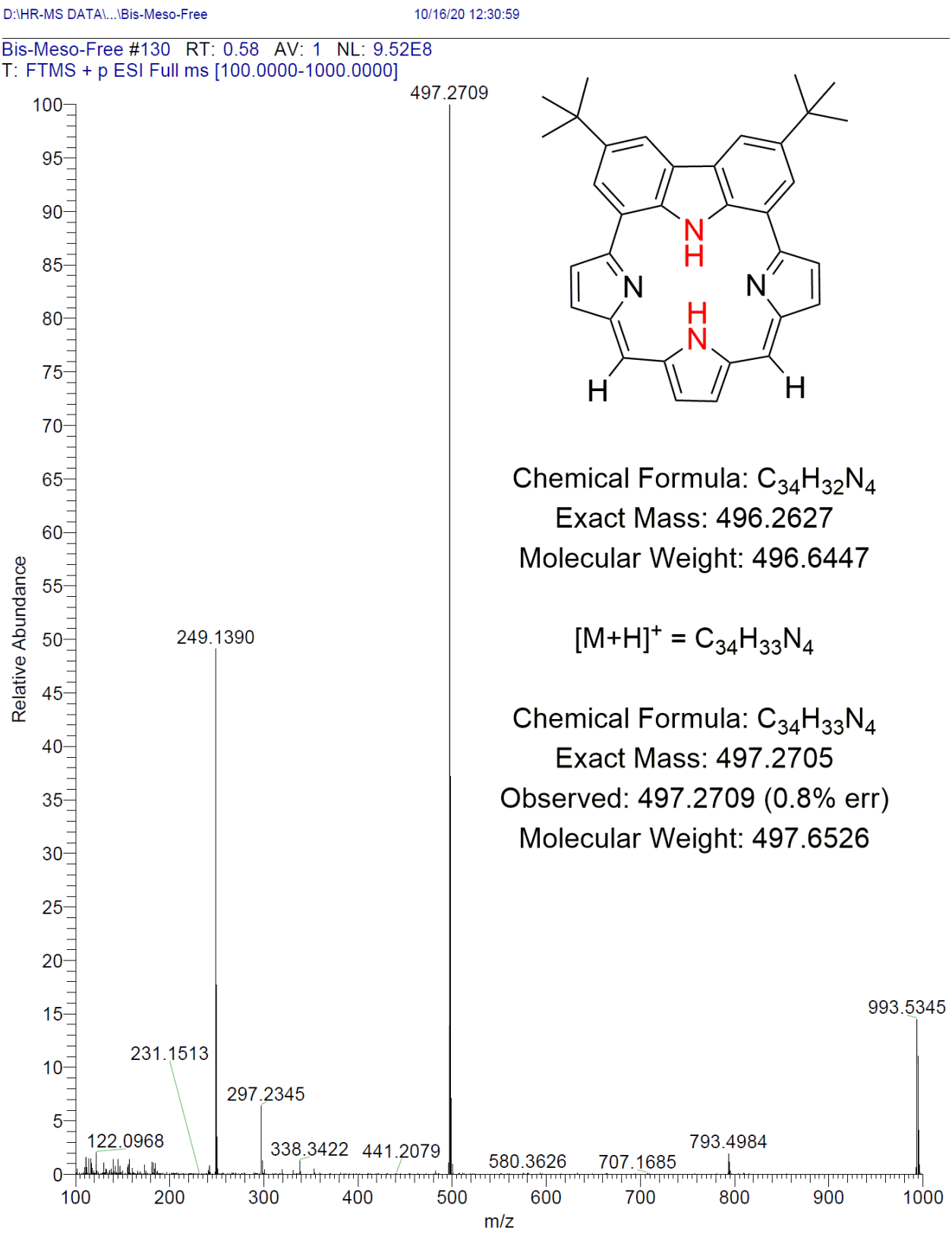

Figure S3.6. HR-MS (ESI) spectrum of **4**.

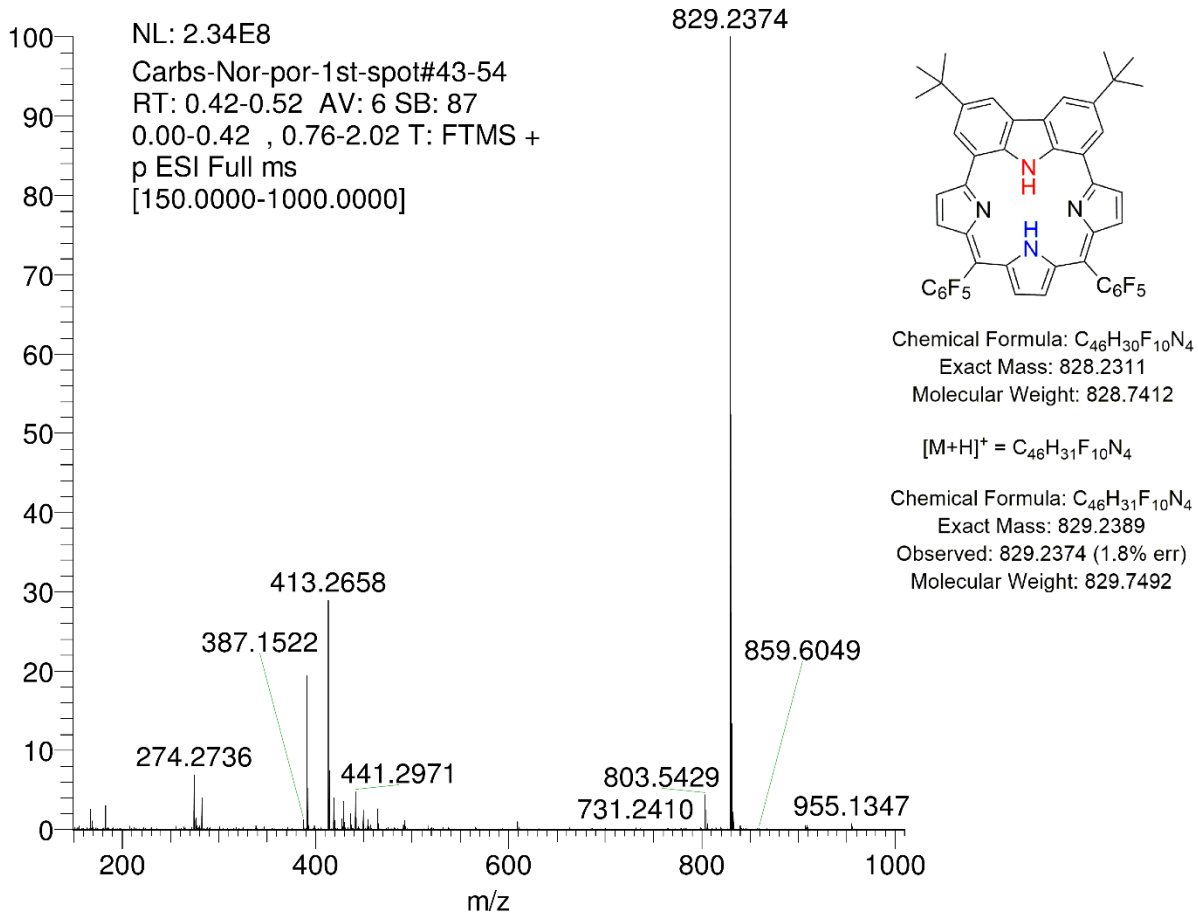

Figure S3.7. HR-MS (ESI) spectrum of **5**.

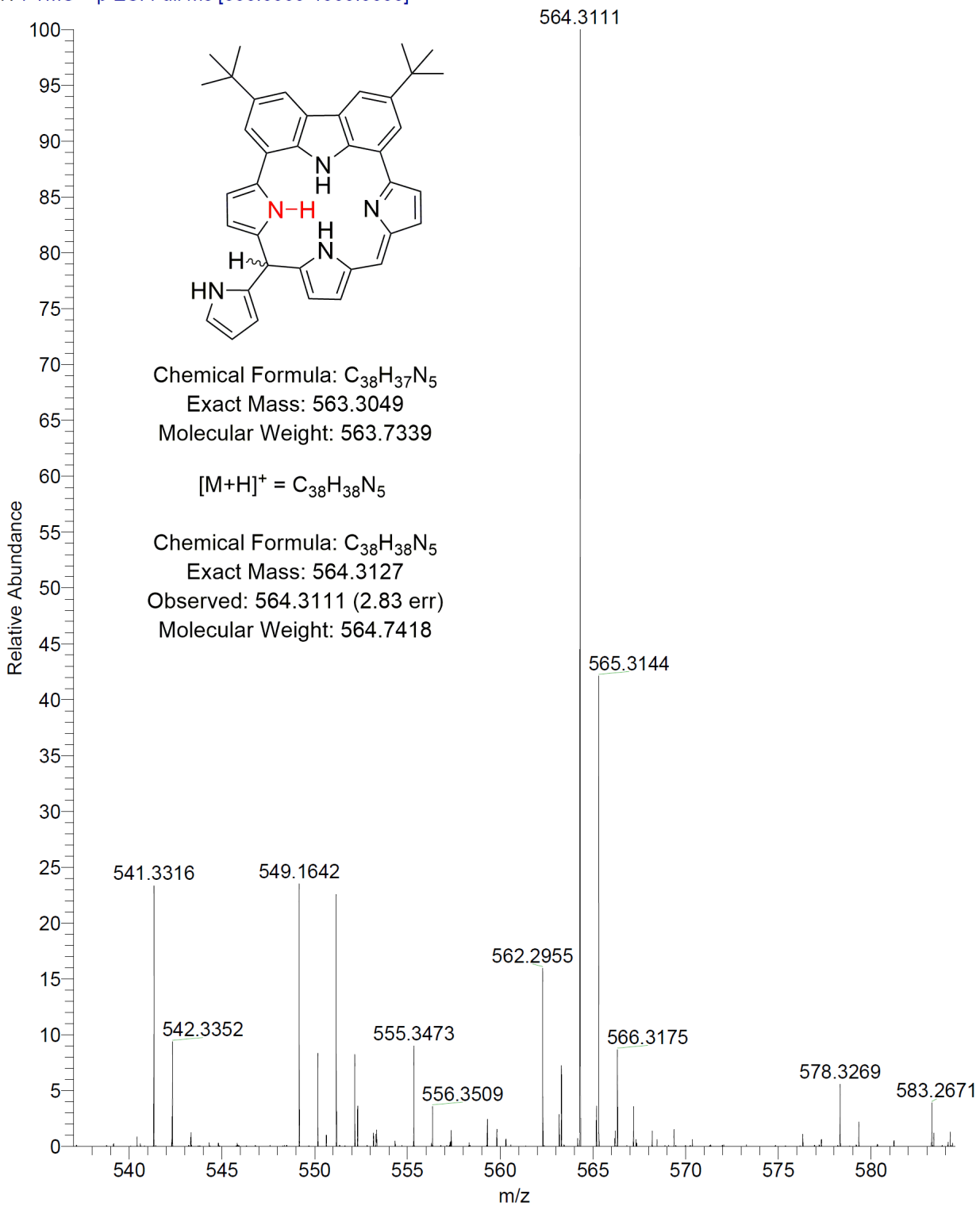

Figure S3.8. HR-MS (ESI) spectrum of **"Route A"** reaction intermediates.

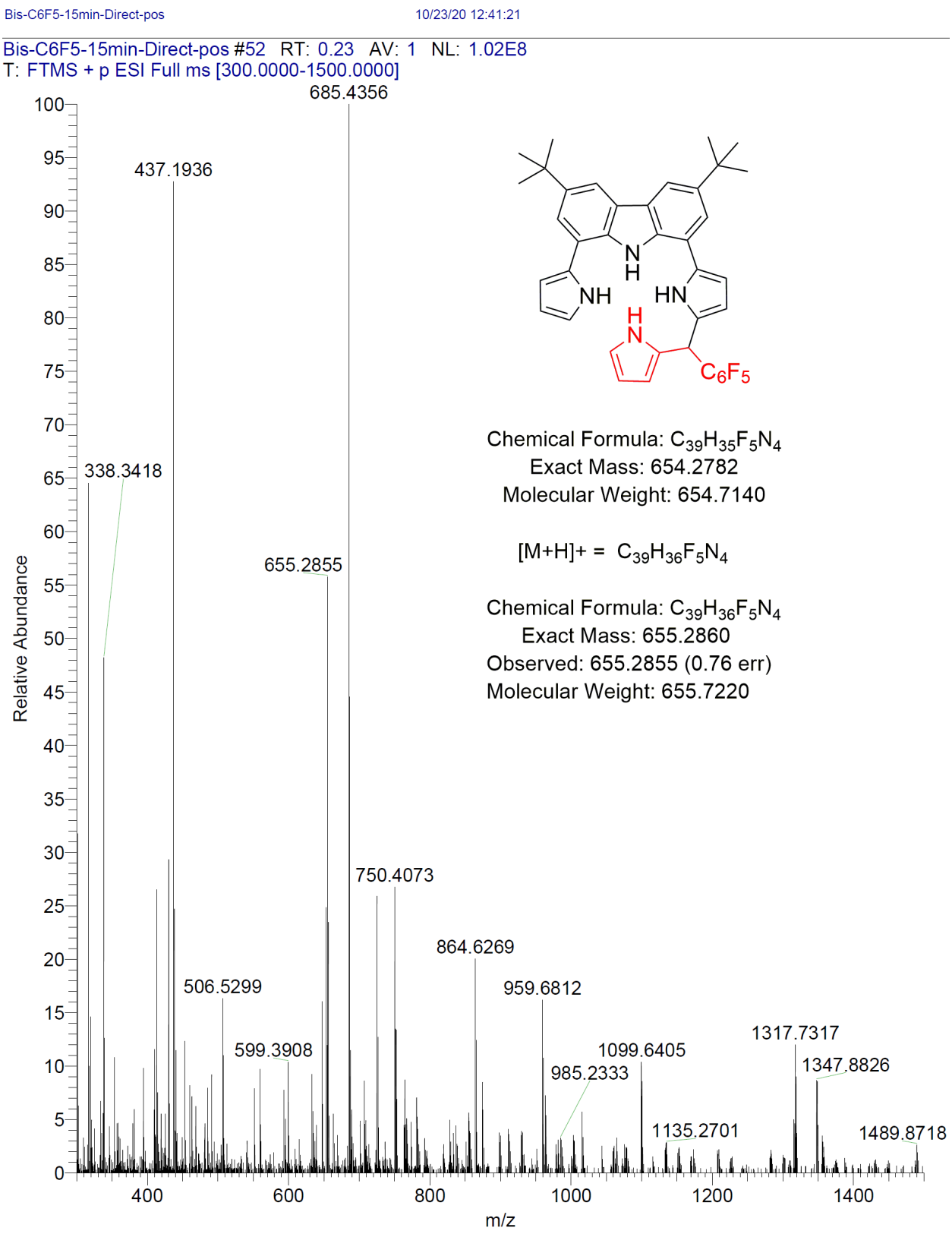

Figure S3.9. HR-MS (ESI) spectrum of **"Route C"** reaction intermediates

4. ^{1}H and ^{13}C NMR Spectra

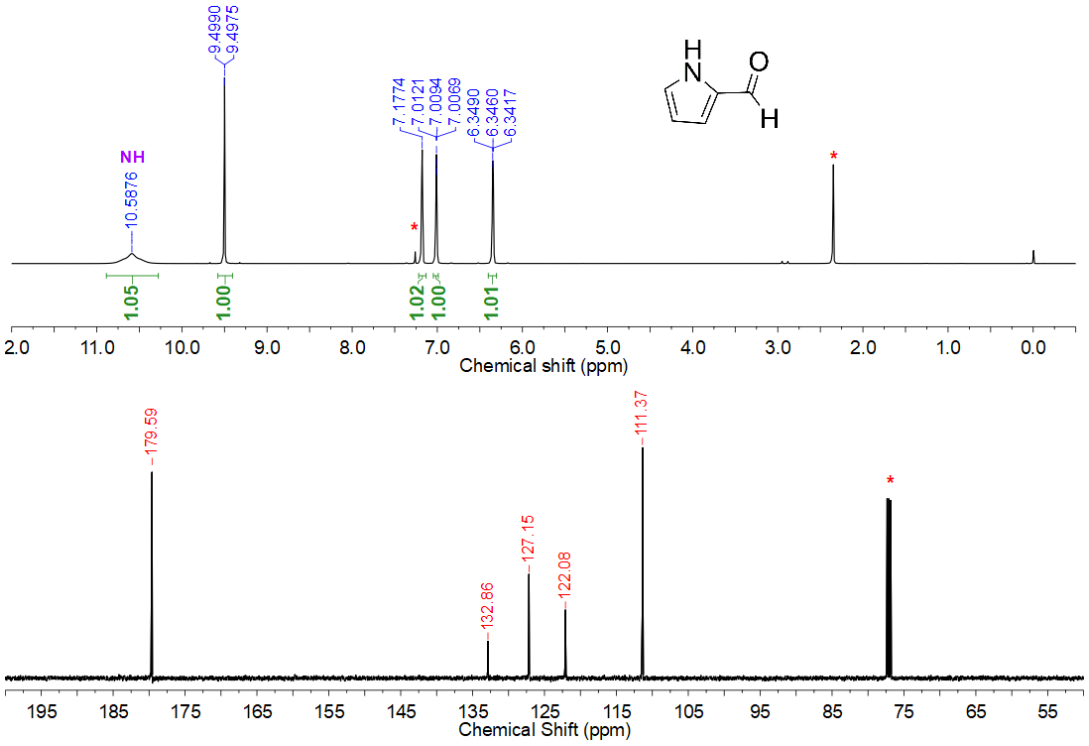

Figure S4.1. ^{1}H (top) and ^{13}C (bottom) NMR spectra of **2a** in $CDCl_3$ at 298 K (500 MHz)

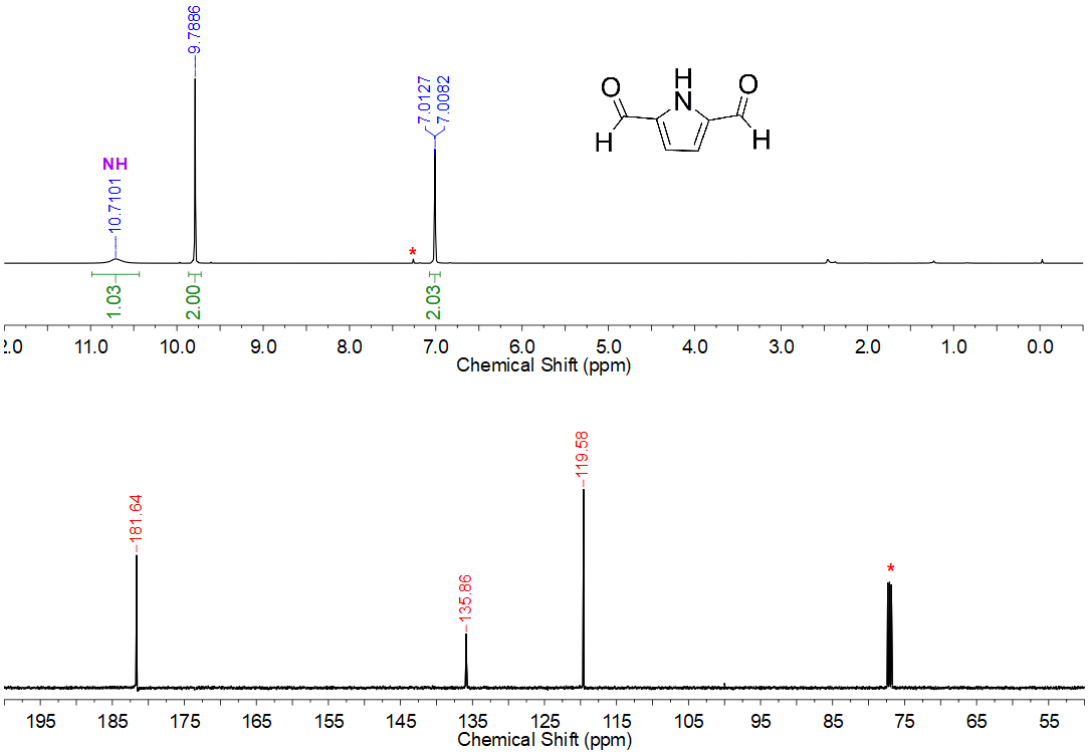

Figure S4.2. ^{1}H (top) and ^{13}C (bottom) NMR spectra of **2b** in $CDCl_3$ at 298 K (500 MHz)

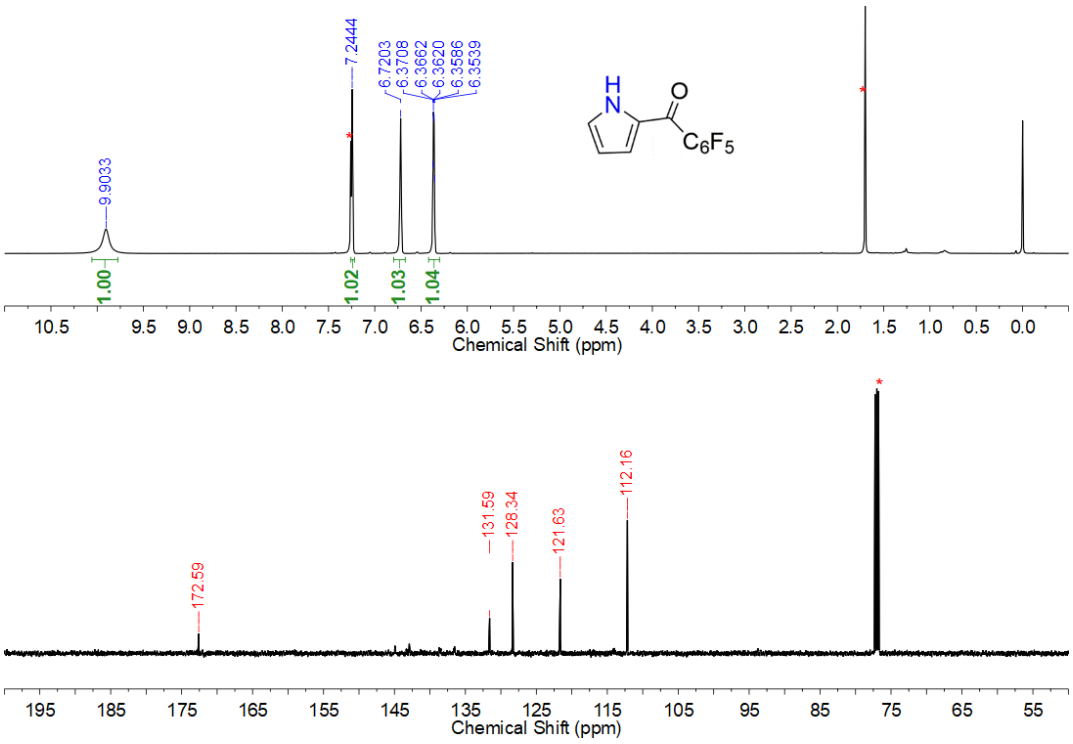

Figure S4.3. ^{1}H (top) and ^{13}C (bottom) NMR spectra of **6** in $CDCl_3$ at 298 K (500 MHz)

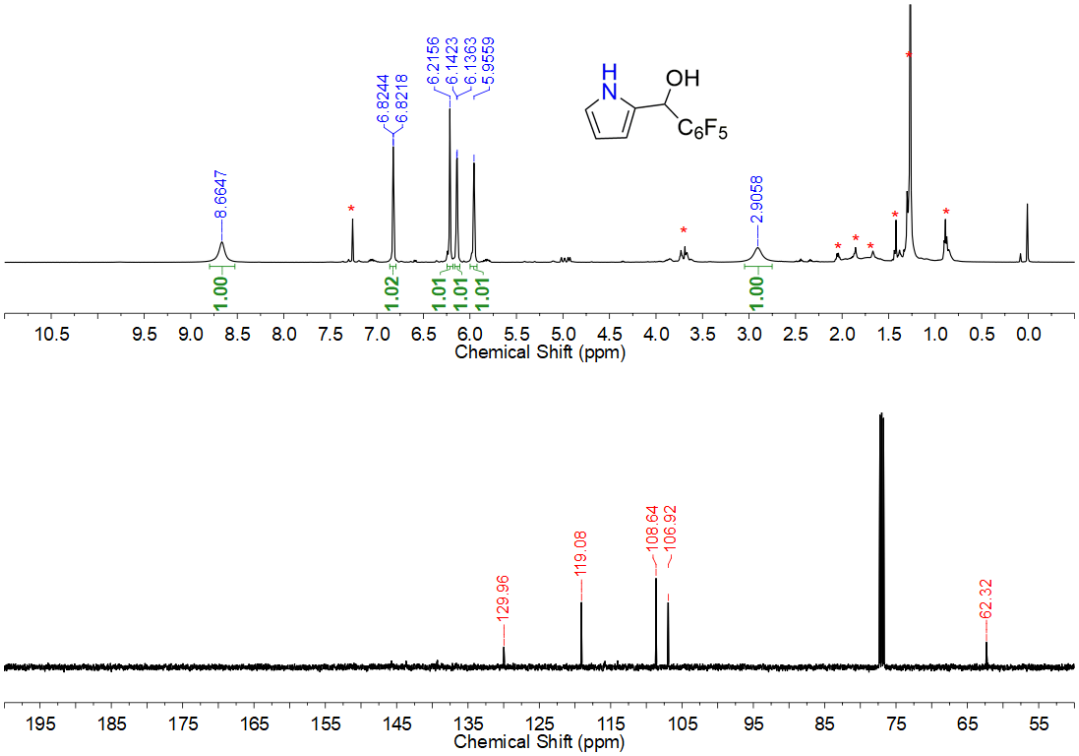

Figure S4.4. ^{1}H (top) and ^{13}C (bottom) NMR spectra of **6a** in $CDCl_3$ at 298 K (500 MHz)

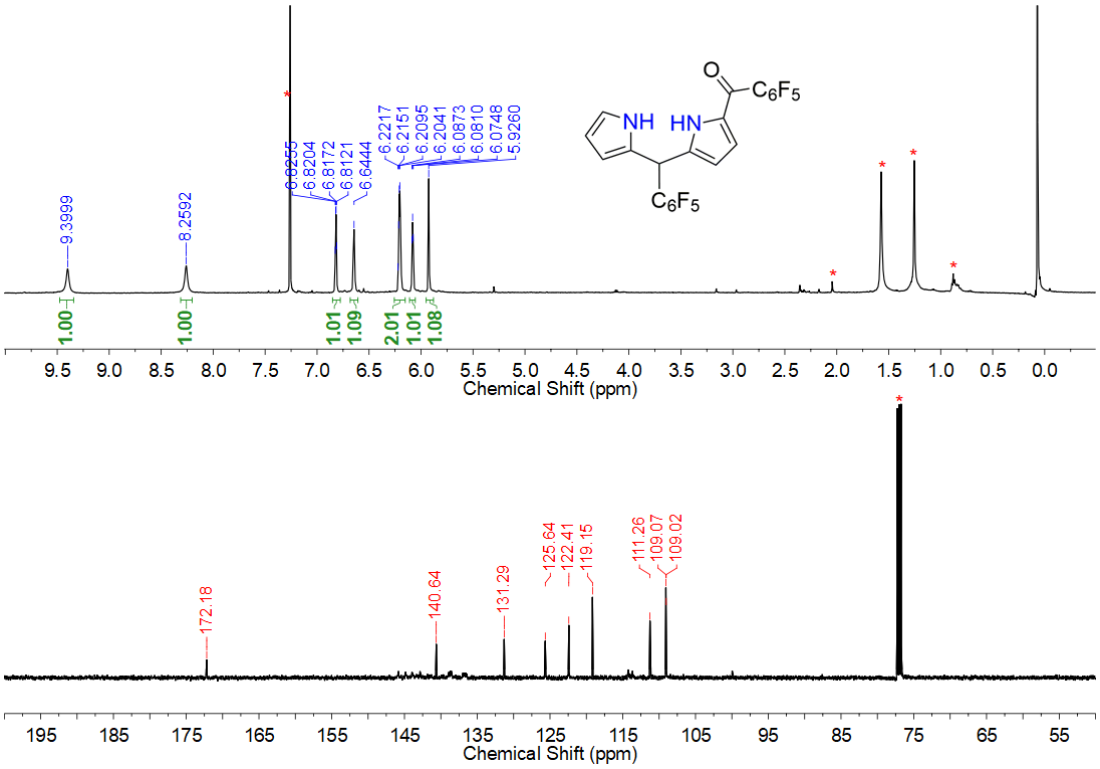

Figure S4.5. ^{1}H (top) and ^{13}C (bottom) NMR spectra of **7** in $CDCl_3$ at 298 K (500 MHz)

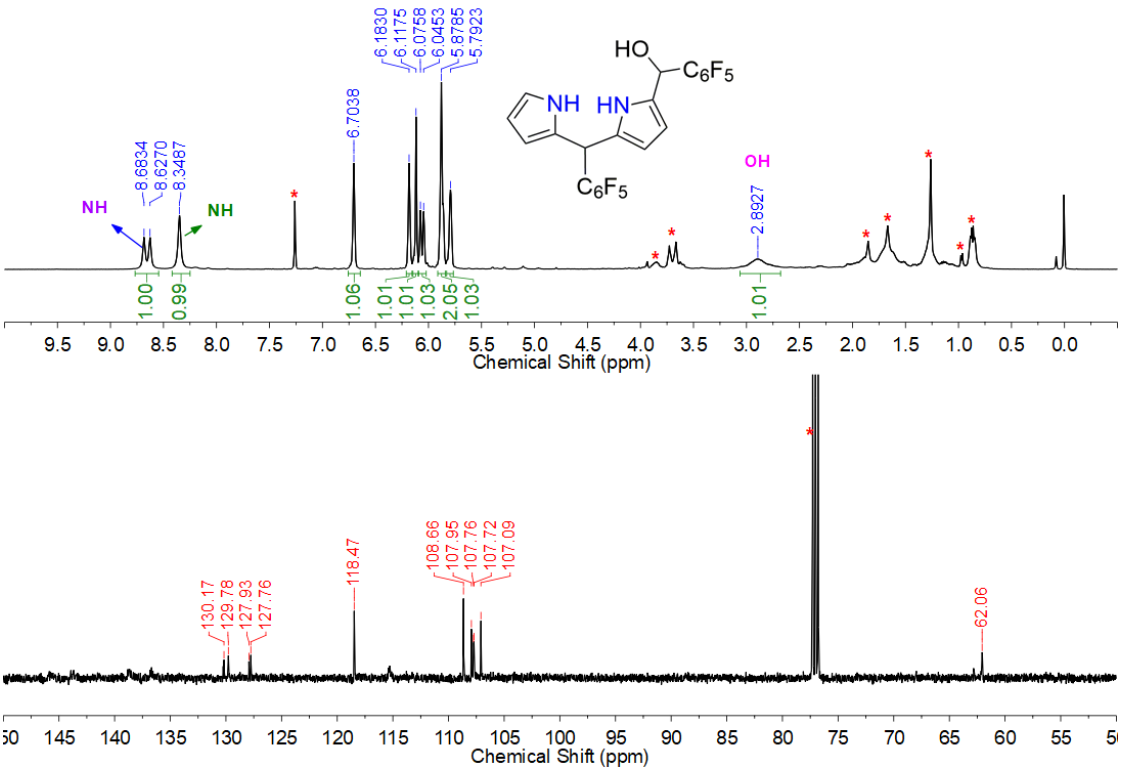

Figure S4.6. ^{1}H (top) and ^{13}C (bottom) NMR spectra of **7a** in $CDCl_3$ at 298 K (500 MHz)

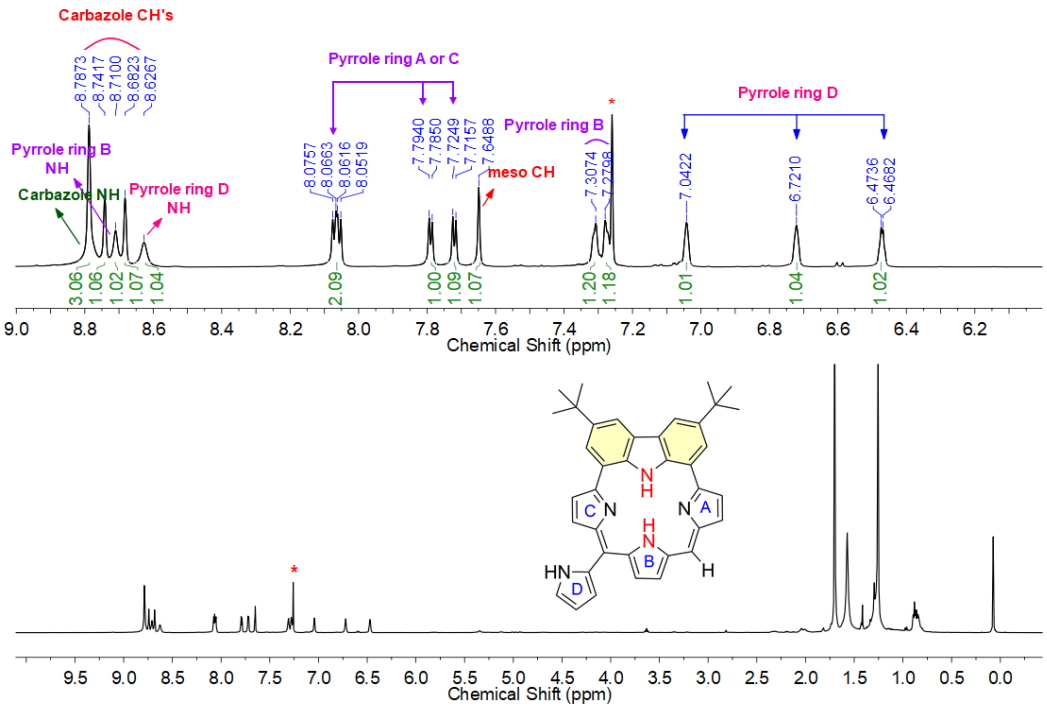

Figure S4.7. ^{1}H NMR spectra of **3** in $CDCl_3$ at 298 K. (500 MHz)

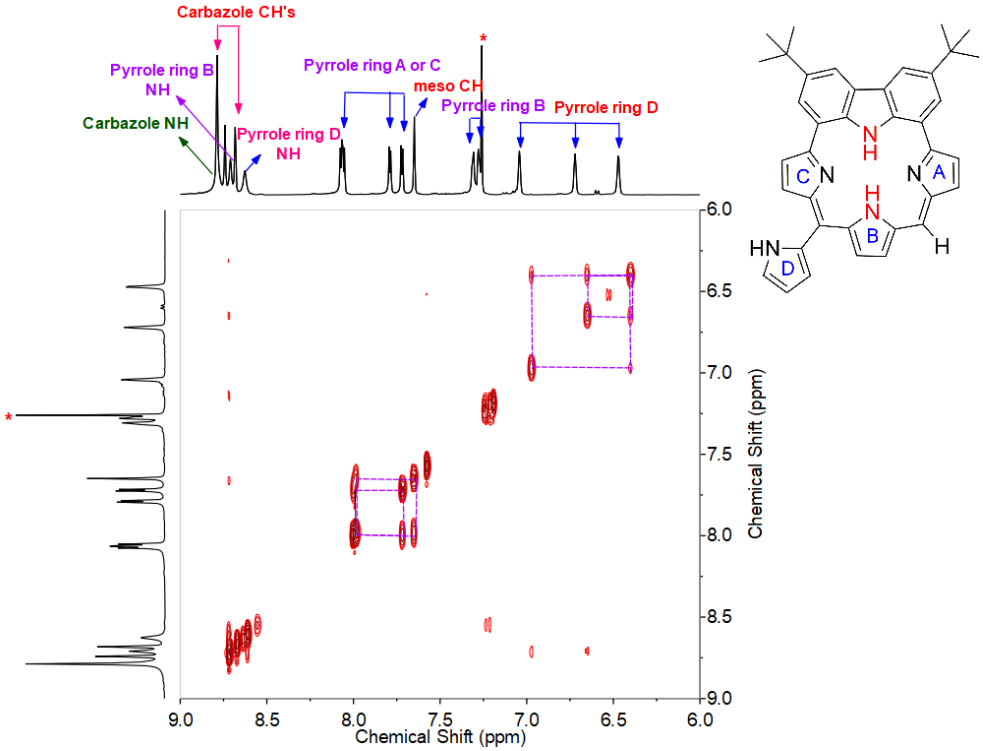

Figure S4.8. ^{1}H-^{1}H COSY spectrum of **3** in $CDCl_3$ at 298 K. (500 MHz)

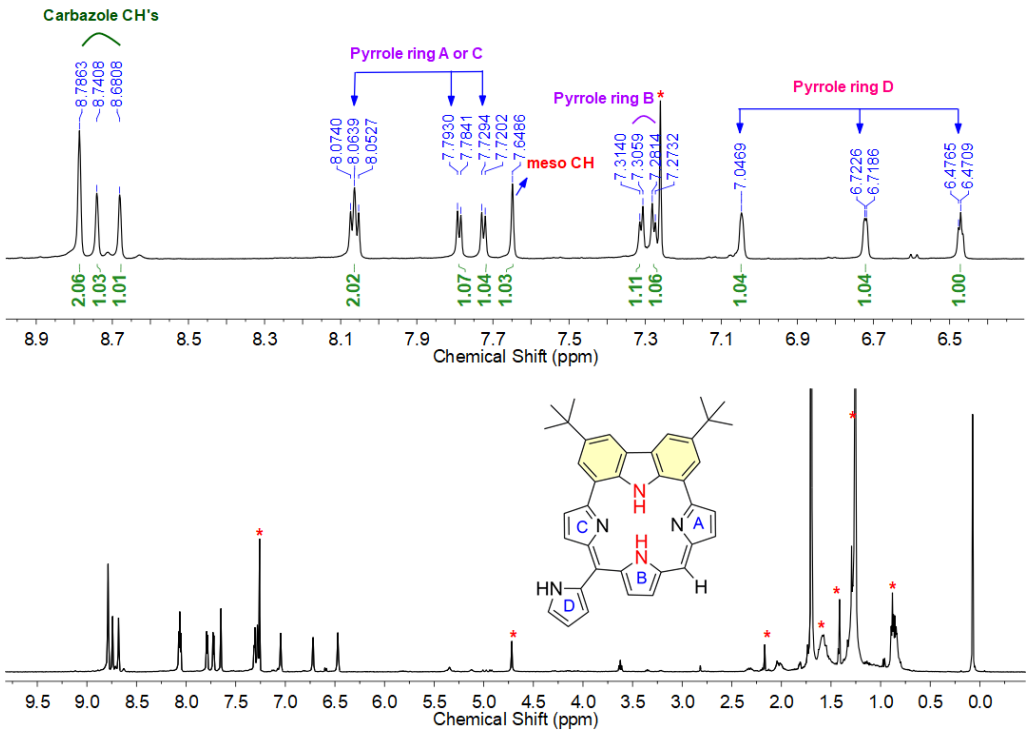

Figure S4.9. ^{1}H NMR spectra of **3** in $CDCl_3$ + D_2O at 298 K. (500 MHz)

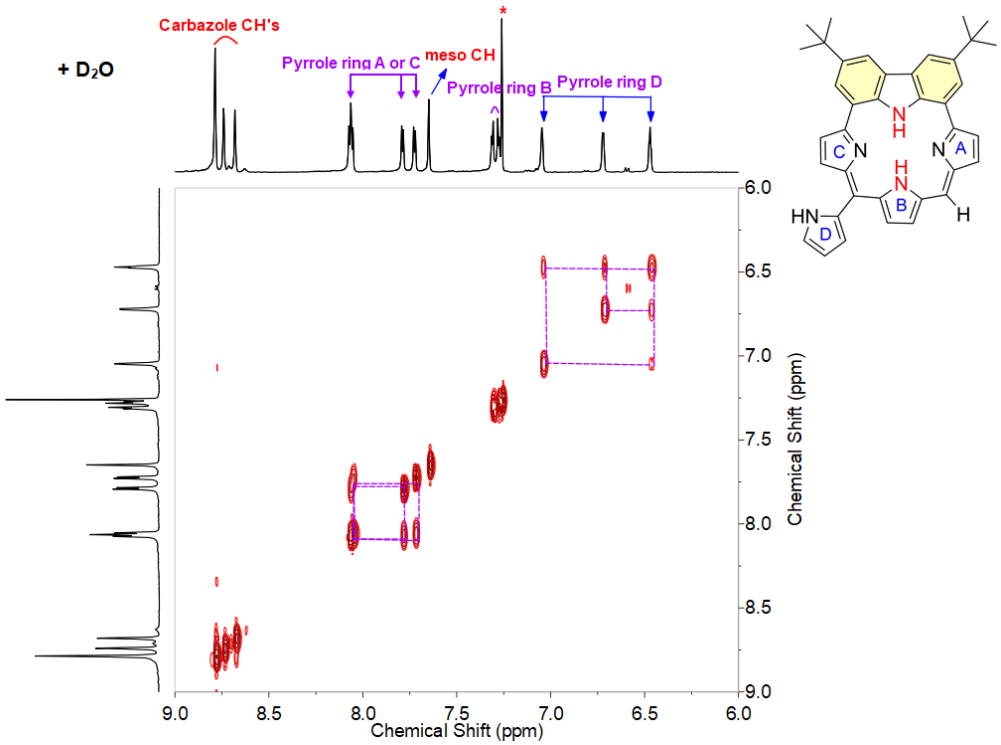

Figure S4.10. ^{1}H-^{1}H COSY spectrum of **3** in $CDCl_3$ + D_2O at 298 K. (500 MHz)

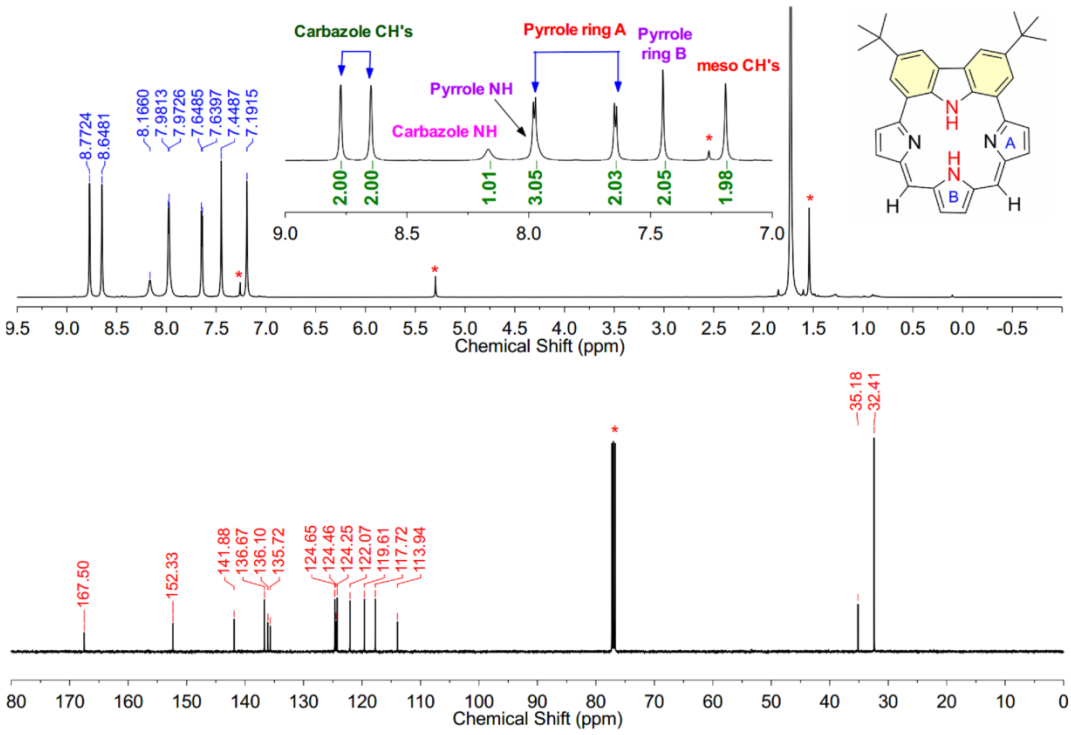

Figure S4.11. ^{1}H (top) and ^{13}C (bottom) NMR spectra of **4** in $CDCl_3$ at 298 K. (500 MHz)

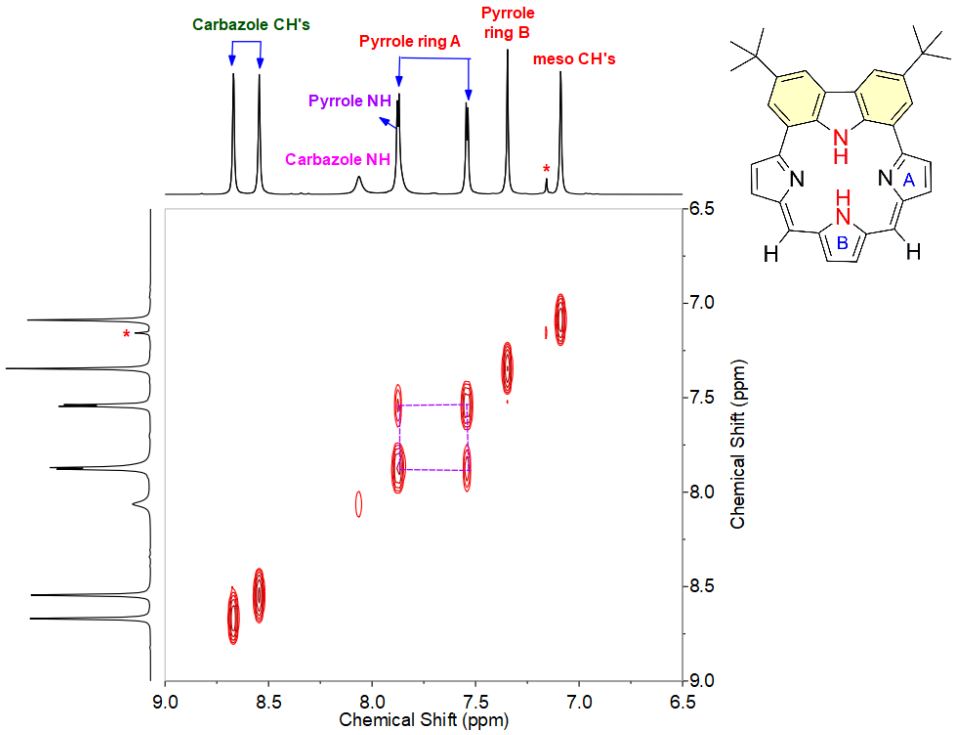

Figure S4.12. ^{1}H-^{1}H COSY spectrum of **4** in $CDCl_3$ at 298 K. (500 MHz)

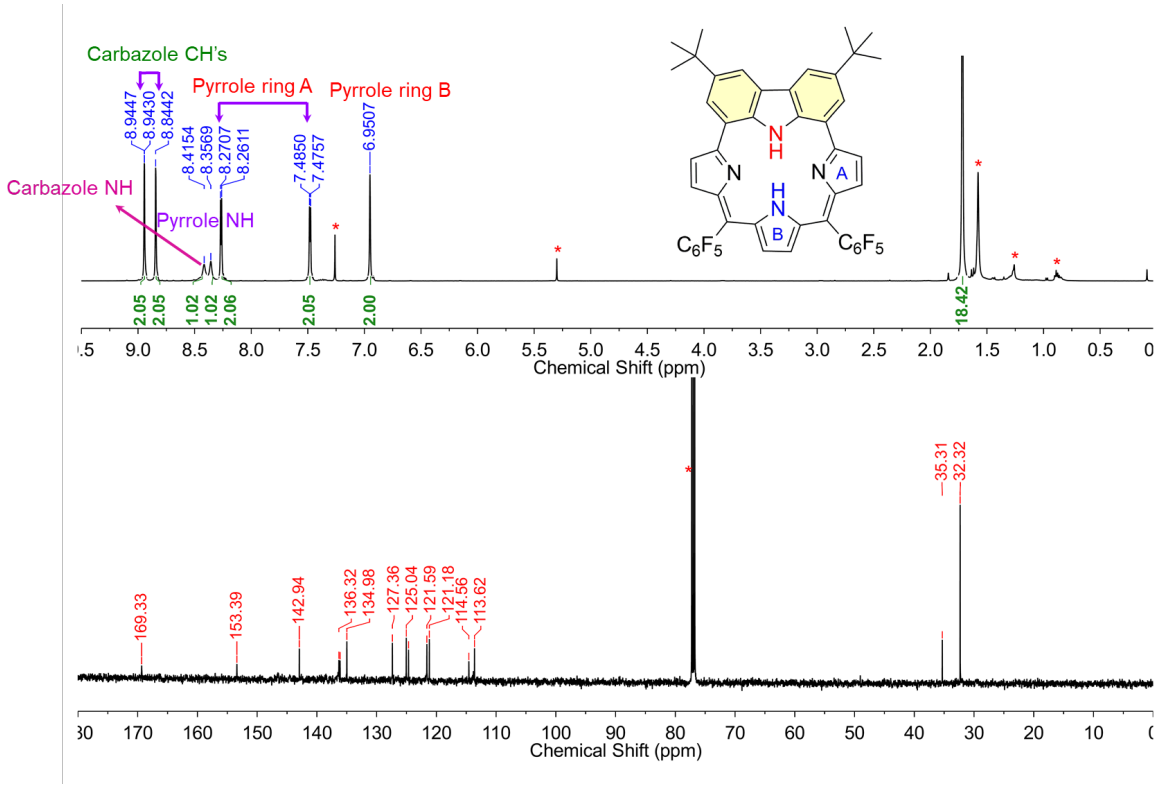

Figure S4.13. ^{1}H (top) and ^{13}C (bottom) NMR spectra of **5** in $CDCl_3$ at 298 K. (500 MHz)

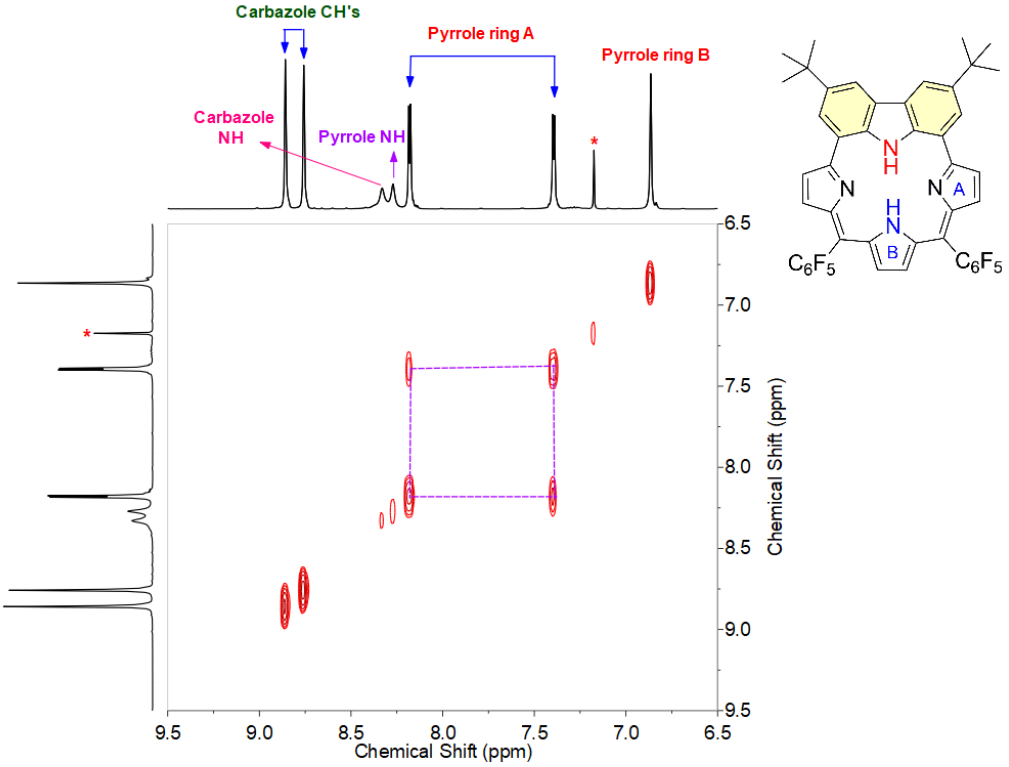

Figure S4.14. ^{1}H-^{1}H COSY spectrum of **5** in $CDCl_3$ at 298 K. (500 MHz)

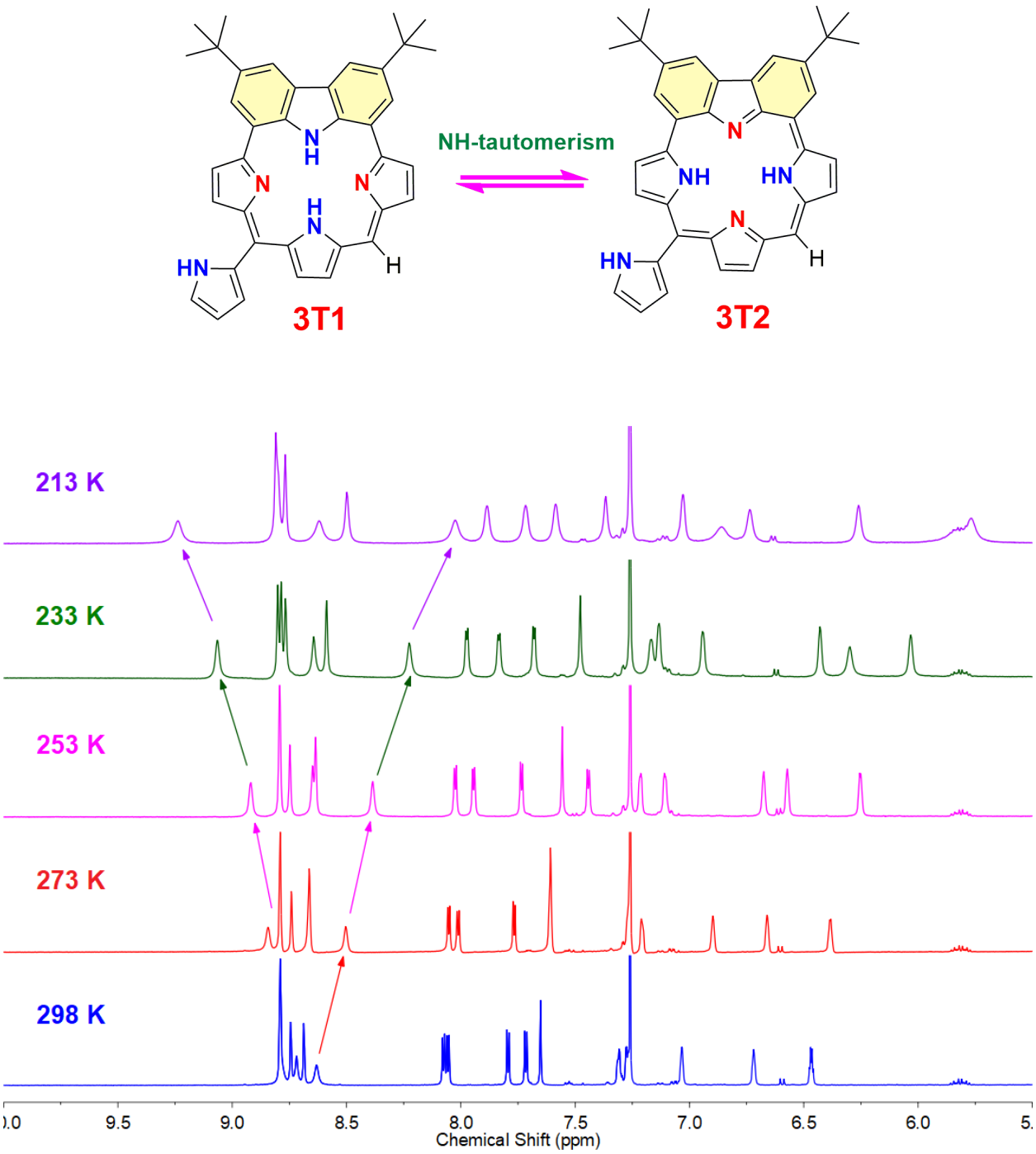

Figure S4.15. ^{1}H NMR spectra of **3** at various temperatures in $CDCl_3$.

5. UV-Vis absorption and emission spectra

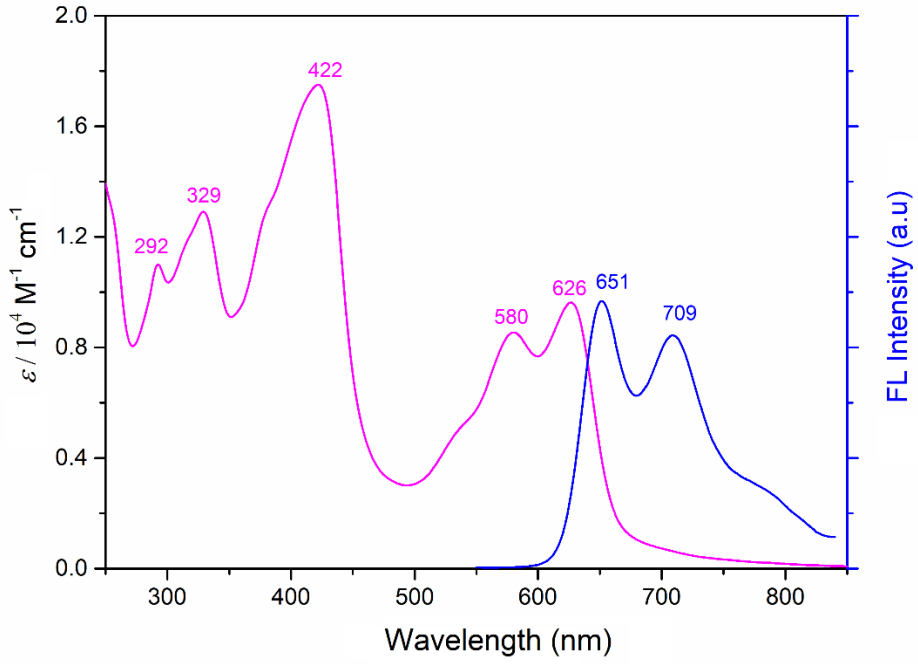

Figure S5.1. UV-Vis absorption spectrum and fluorescence spectrum of **3** recorded in CH_2Cl_2. (λ_{ex} = 440 nm)

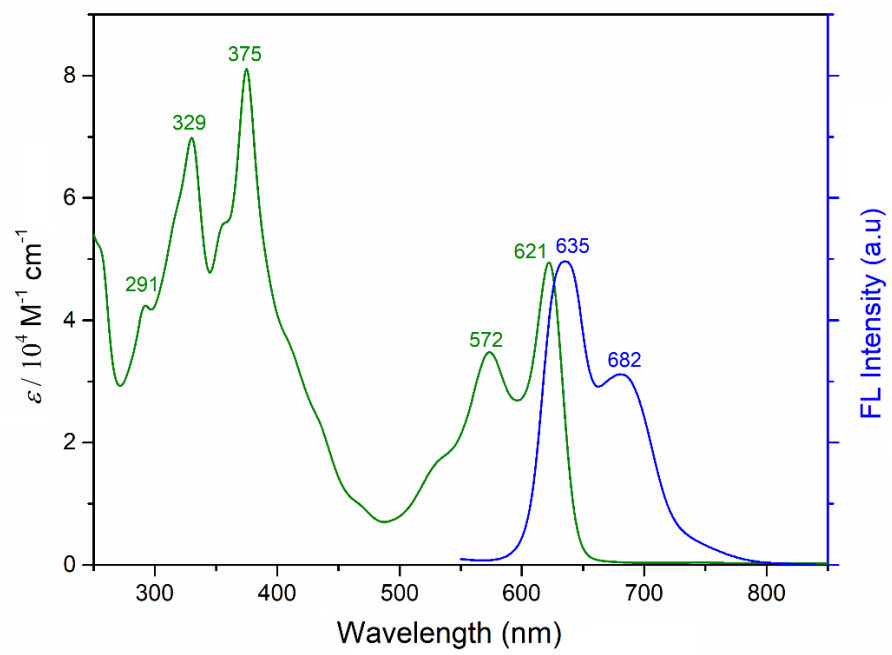

Figure S5.2. UV-Vis absorption spectrum and fluorescence spectrum of **4** recorded in CH_2Cl_2. (λ_{ex} = 440 nm)

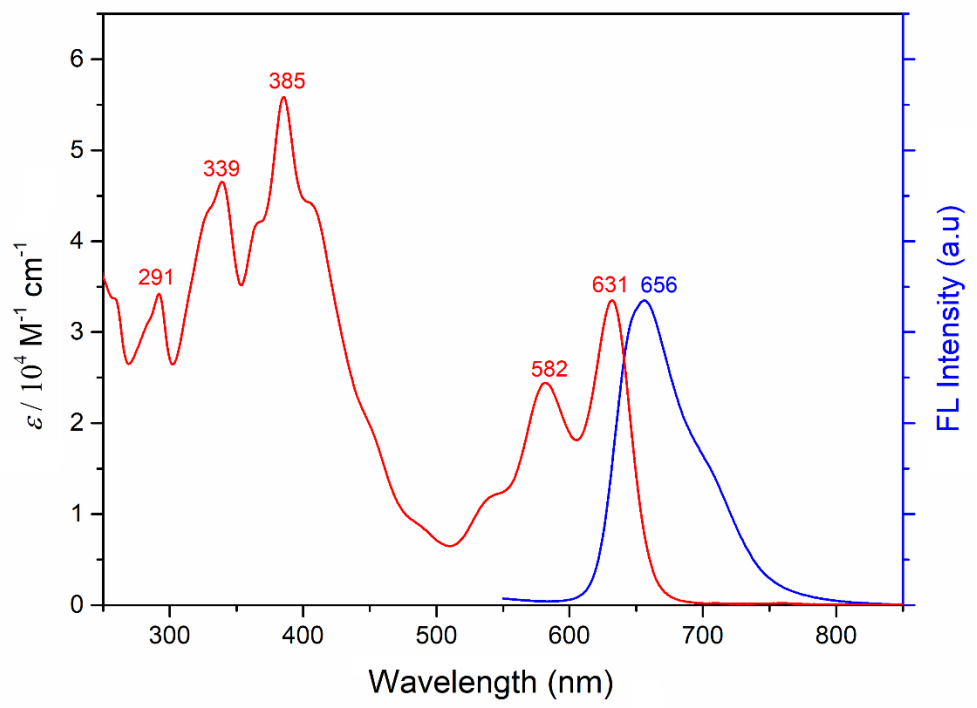

Figure S5.3. UV-Vis absorption spectrum and fluorescence spectrum of **5** recorded in CH_2Cl_2. (λ_{ex} = 440 nm)

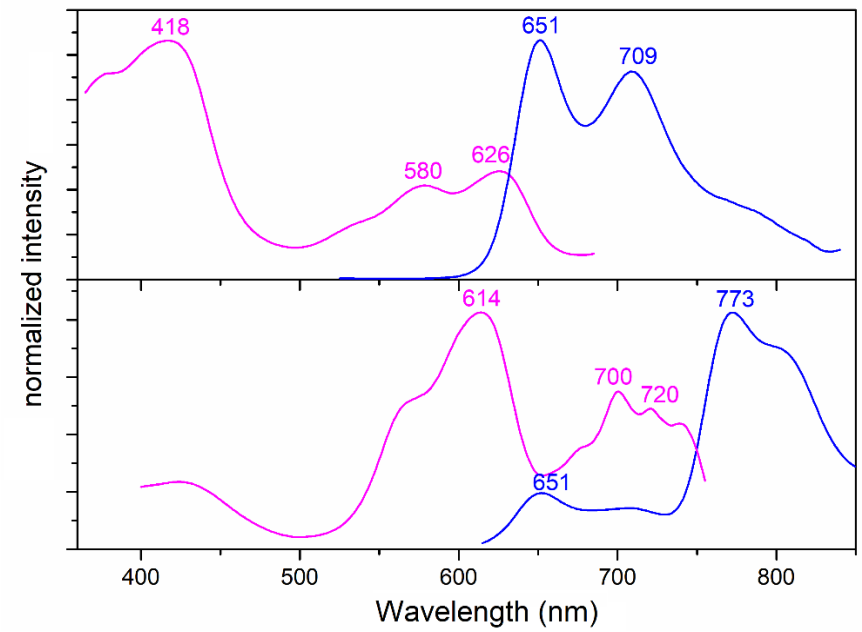

Figure S5.4. (a) Excitation spectra (magenta) of **3** detected at λ_{em} = 651 nm and fluorescence spectra (blue) of **3** excited at 420 nm (b) Excitation spectra (magenta) of **3** detected at λ_{em} = 773 nm and fluorescence spectrum (blue) of **3** excited at 610 nm in CH_2Cl_2.

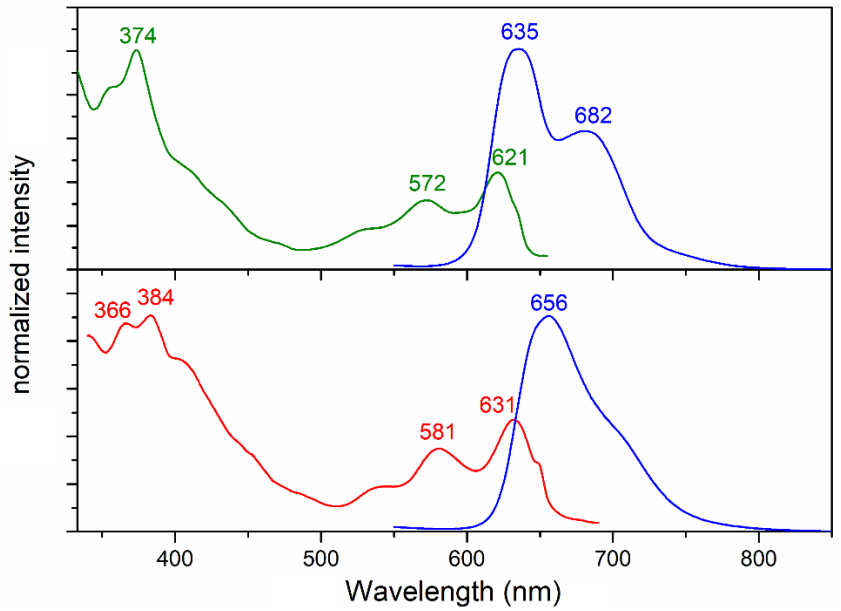

Figure S5.5. (a) Excitation spectra (green) of **4** detected at λ_{em} = 635 or 683 nm and fluorescence spectra (blue) of **4** excited at 440 nm (b) Excitation spectra (red) of **5** detected at λ_{em} = 635 and fluorescence spectrum (blue) of **5** excited at 440 nm in CH_2Cl_2.

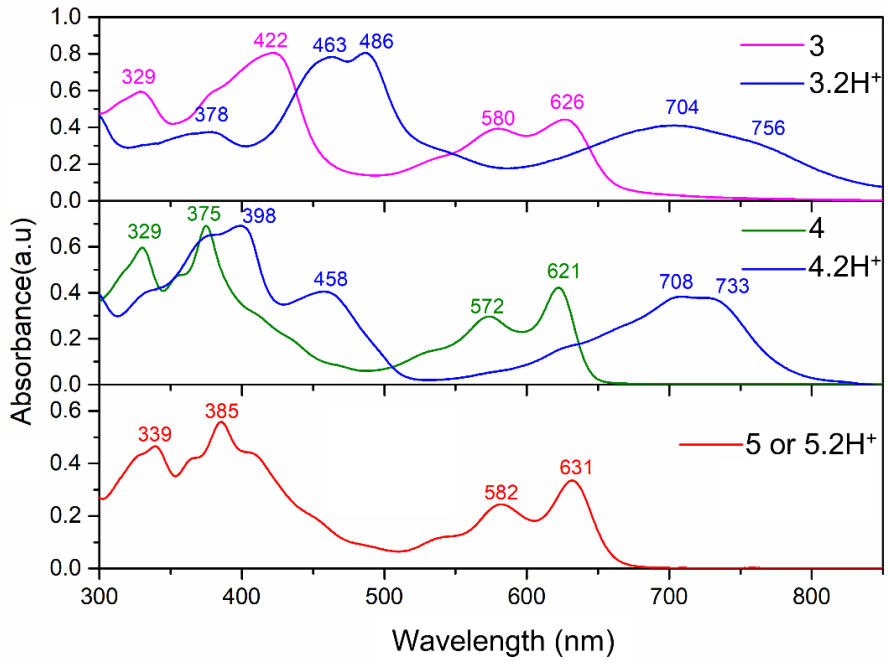

Figure S5.6. Absorption spectra of **3**, **4** and **5** (from top) along with their protonated forms in CH_2Cl_2. Protonation was achieved by adding diluted CF_3COOH into the corresponding freebase in CH_2Cl_2. *Spectral features remains same even after excess addition of CF_3COOH in **5**.

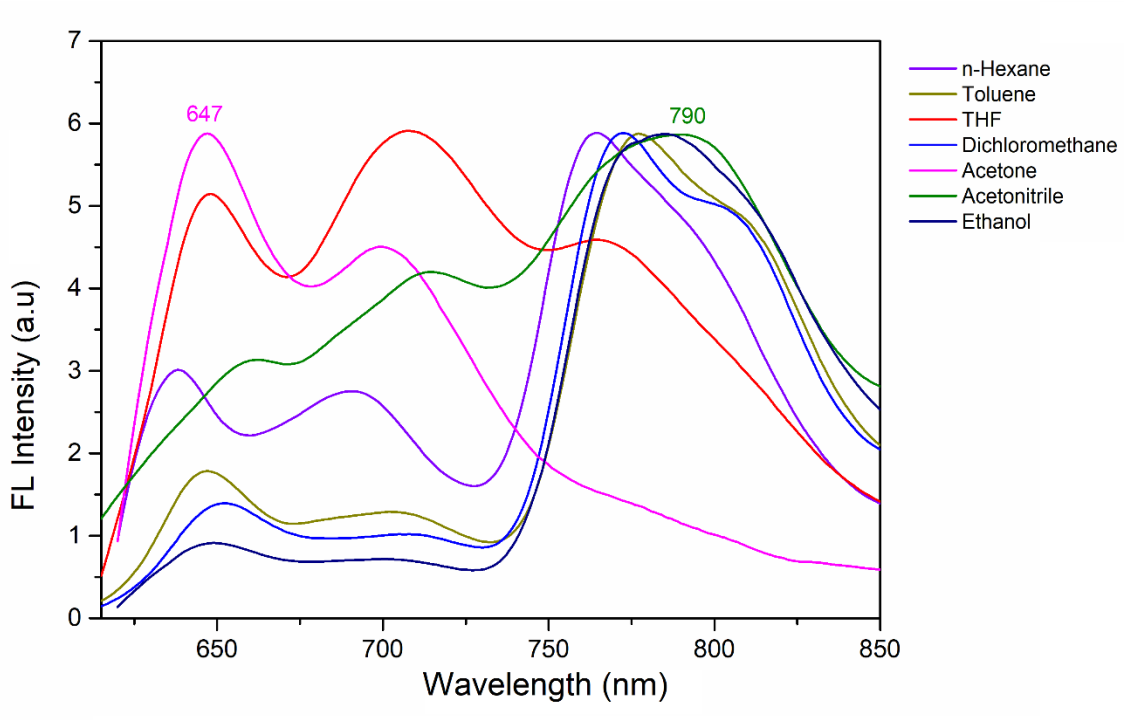

Figure S5.7. Emission spectra of **3** recorded in different solvents and excited at 600 nm.

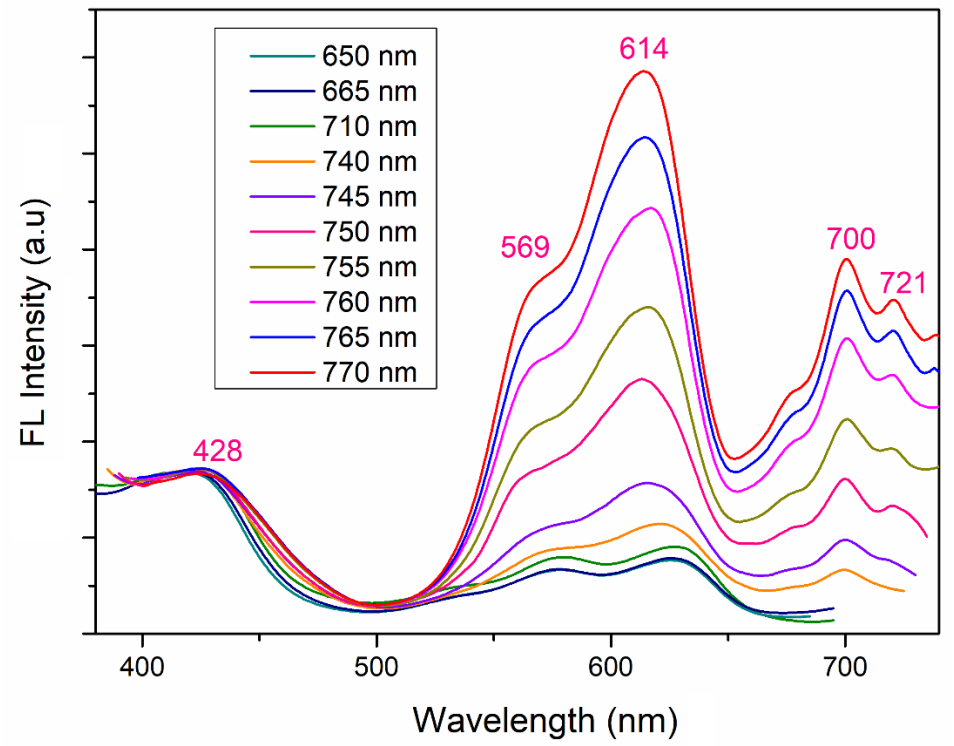

Figure S5.8. Excitation spectra of **3** detected at various emission wavelengths (λ_{em} = 650-770 nm) in CH_2Cl_2.

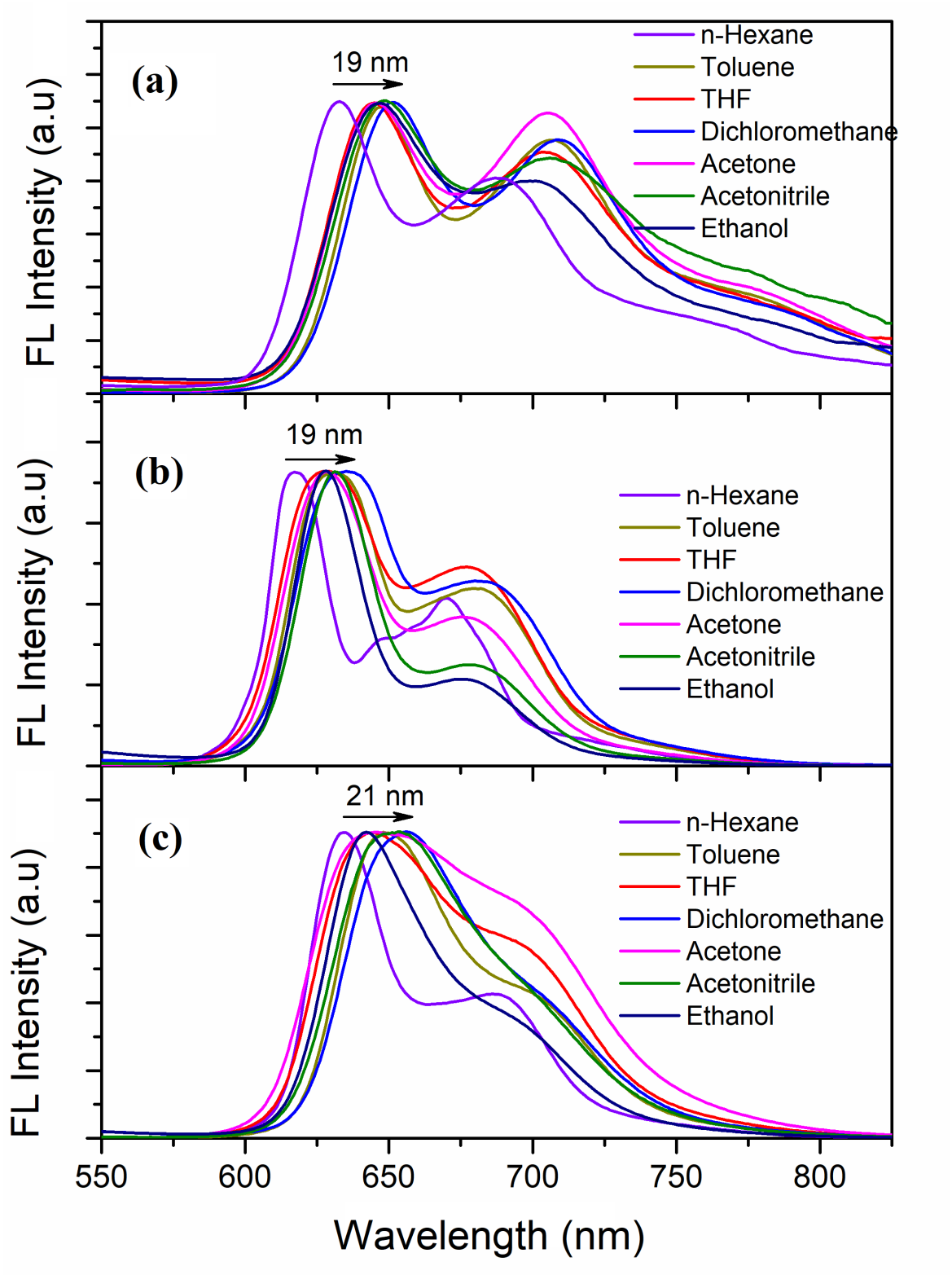

Figure S5.9. Emission spectra of (a) **3** (b) **4** and (c) **5** recorded in different solvents and excited at 440 nm.

6. X-ray Crystallographic Details

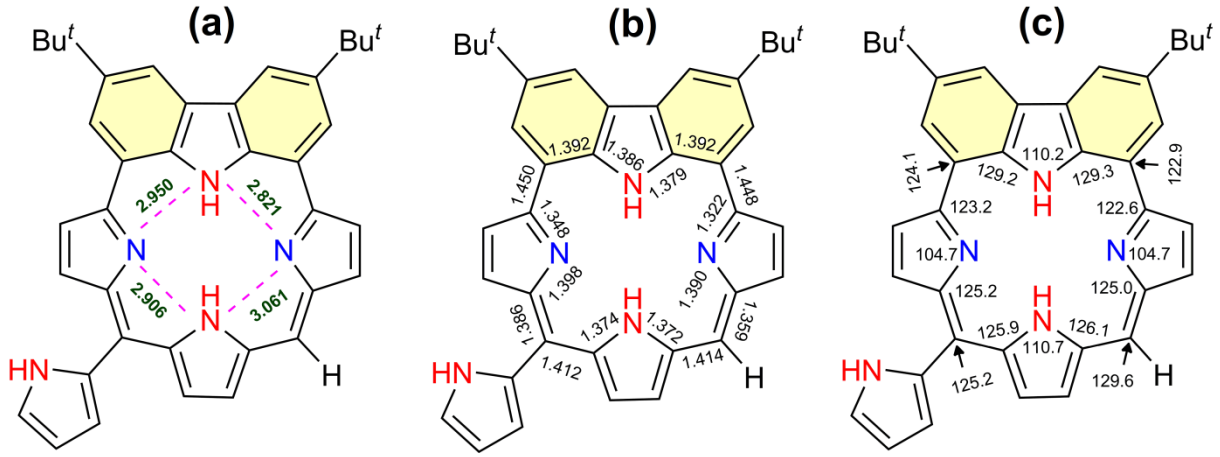

Figure S6.1. (a) and (b) Selected bond lengths (Å) and (c) bond angles (°) of **3**.

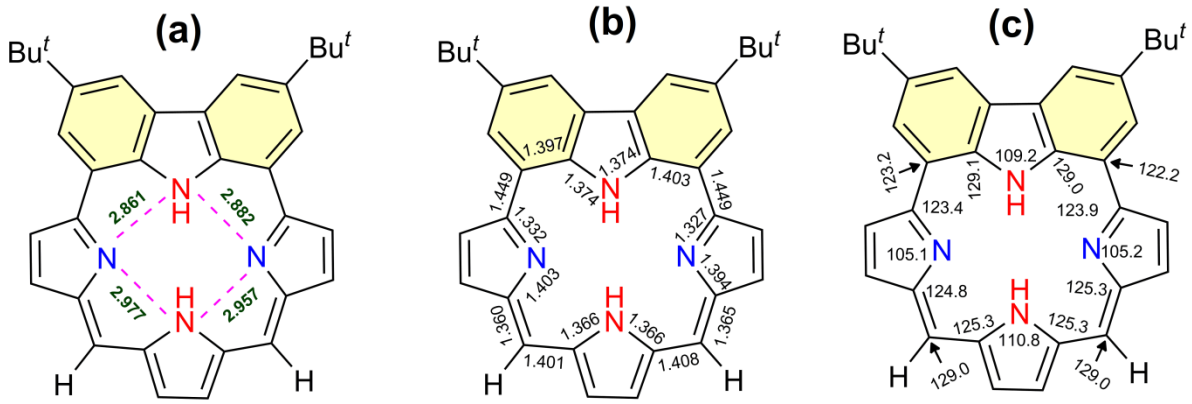

Figure S6.2. (a) and (b) Selected bond lengths (Å) and (b) bond angles (°) of **4**.

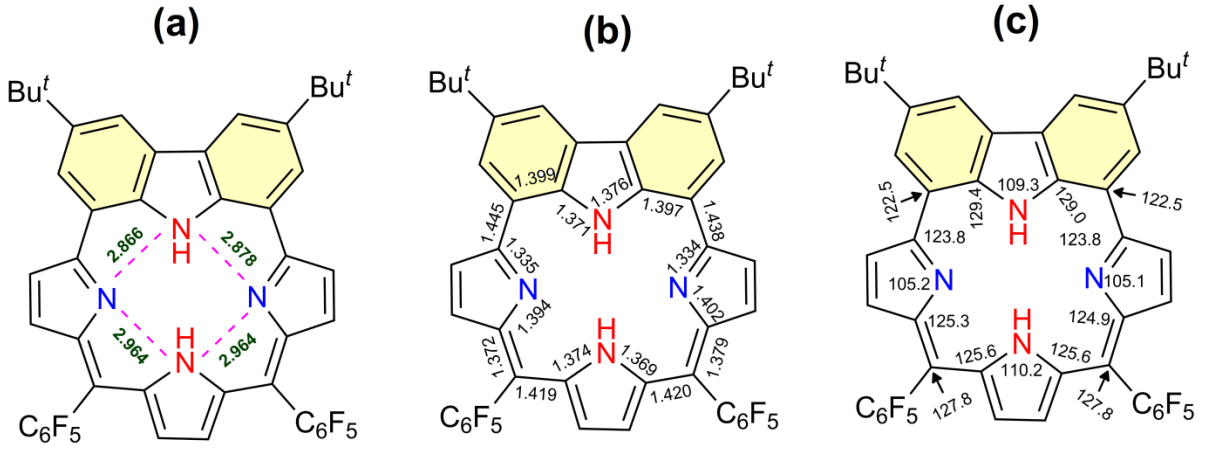

Figure S6.3. (a) and (b) Selected bond lengths (Å) and (b) bond angles (°) of **5**.

Table S6.2. Crystal data and structure refinements for 3

Compound	**3**
Formula	$C_{152}H_{139}N_{20}$
M_w	2245.82
Temperature/K	296(2) K
Crystal system	Triclinic
Space group	P-1
a/Å	17.34(11)
b/Å	19.29(12)
c/Å	20.34(12)
α/°[deg]	78.751(2)
β/°[deg]	86.794(2)
γ/°[deg]	82.449(2)
Volume[$Å^3$]	6618.8(7)
Z	2
ρ_{calc}[Mg/m^3]	1.127
μ/mm^{-1}	0.067
F(000)	2382
Crystal size/mm^3	0.240 x 0.200 x 0.150
Radiation	MoKα (λ = 0.71073)
2Θ range for data collection/°	1.341 to 24.999
Reflections collected	156625
Goodness-of-fit on F^2	1.013
Final R indexes [I>=2σ (I)]	R1 = 0.0668, wR2 = 0.1716
Final R indexes [all data]	R1 = 0.1637, wR2 = 0.2351
Largest diff. peak/hole / e $Å^{-3}$	0.256/-0.221
Solvent System	Toluene/CH_3OH
CCDC	2062803

Table S6.3. Crystal data and structure refinements for 4 and 5

Compound	**4**	**5**
Formula	$C_{34}H_{32}N_4$	$C_{46}H_{30}F_{10}N_4$
M_w	496.63	828.74
Temperature/K	296(2) K	296(2)
Crystal system	monoclinic	monoclinic
Space group	P 2_1/n	P2_1/c
a/Å	15.32(10)	15.15(15)
b/Å	10.13(7)	11.59(11)
c/Å	17.75(11)	22.24(2)
α/°[deg]	90	90
β/°[deg]	103.791(3)	99.375(3)
γ/°[deg]	90	90
Volume[Å^3]	2679.5(3)	3857.7(7)
Z	4	4
ρ_{calc}[Mg/m^3]	1.231	1.427
μ/mm^{-1}	0.073	0.118
F(000)	1056	1696
Crystal size/mm^3	0.250 x 0.230 x 0.180	0.200 x 0.200 x 0.120
Radiation	MoKα (λ = 0.71073)	MoKα (λ = 0.71073)
2Θ range for data collection/°	2.330 to 26.000	2.321 to 25.999
Reflections collected	39985	45894
Goodness-of-fit on F^2	1.044	0.999
Final R indexes [I>=2σ (I)]	R1 = 0.0517, wR2 = 0.1252	R1 = 0.0509, wR2 = 0.1067
Final R indexes [all data]	R1 = 0.1050, wR2 = 0.1613	R1 = 0.1284, wR2 = 0.1453
Largest diff. peak/hole / e Å^{-3}	0.267/-0.189	0.195/-0.274
Solvent System	$CHCl_3$/CH_3OH	$CHCl_3$/CH_3OH
CCDC	2059574	2059575

7. Computational Studies[S1]

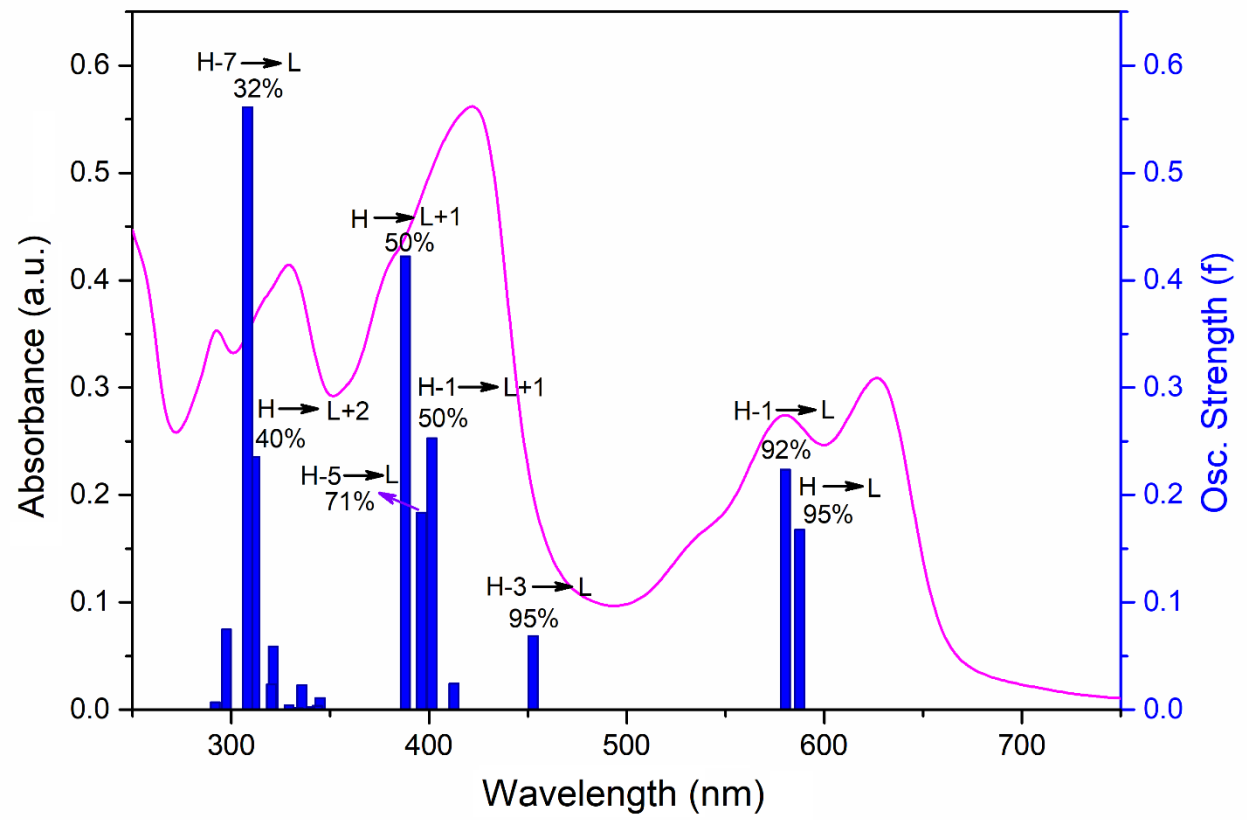

Figure S7.1. Calculated oscillator strength on the basis of optimized structure (bar) and observed absorption spectra (line) of **3**.

Table S7.1: Transition energies, oscillator strength and orbital contributions calculated for **3** from TDDFT analysis at (TD)B3LYP/6-31g(d) level of theory (H = HOMO, L= LUMO)

Transition	Wavelength (nm)	Oscillator Strength (f)	Major Contributions
$S_0 \rightarrow S_1$	587.45	0.1676	H→ L (94.78%)
$S_0 \rightarrow S_2$	580.27	0.2235	H-1 → L(91.84%)
$S_0 \rightarrow S_3$	484.88	0.0004	H-2 →L (96.36%)
$S_0 \rightarrow S_4$	452.58	0.0688	H-3 → L (94.91%)
$S_0 \rightarrow S_5$	412.65	0.0244	H-4 → L (84.84%)
$S_0 \rightarrow S_6$	401.43	0.2528	H-1 → L+1(50.53%) H-5 → L (22.01%)
$S_0 \rightarrow S_7$	396.24	0.1837	H-5 → L (71.24%)
$S_0 \rightarrow S_8$	387.90	0.4221	H → L+1 (50.65%) H-1 → L+1 (22.54%)

$S_0 \rightarrow S_9$	344.90	0.0111	H-6 → L (68.95%)
$S_0 \rightarrow S_{10}$	343.46	0.0037	H-2 → L+1 (66.99%)
$S_0 \rightarrow S_{11}$	339.51	0.0024	H-10 → L (59.19%)
$S_0 \rightarrow S_{12}$	335.63	0.0230	H-3 → L+1 (73.56%)
$S_0 \rightarrow S_{13}$	333.66	0.0016	H-11 → L (78.10%)
$S_0 \rightarrow S_{14}$	329.12	0.0042	H-8 → L (46.56%) H → L+2 (30.38%)
$S_0 \rightarrow S_{15}$	321.12	0.0588	H-1 → L+2 (68.73%)
$S_0 \rightarrow S_{16}$	320.22	0.0236	H-9 → L (61.39%)
$S_0 \rightarrow S_{17}$	311.85	0.2355	H → L+2 (40.33%)
$S_0 \rightarrow S_{18}$	308.09	0.5613	H-7 → L (32.16%)
$S_0 \rightarrow S_{19}$	297.49	0.0747	H-4 → L+1 (79.99%)
$S_0 \rightarrow S_{20}$	291.83	0.0069	H-5 → L+1 (87.11%)

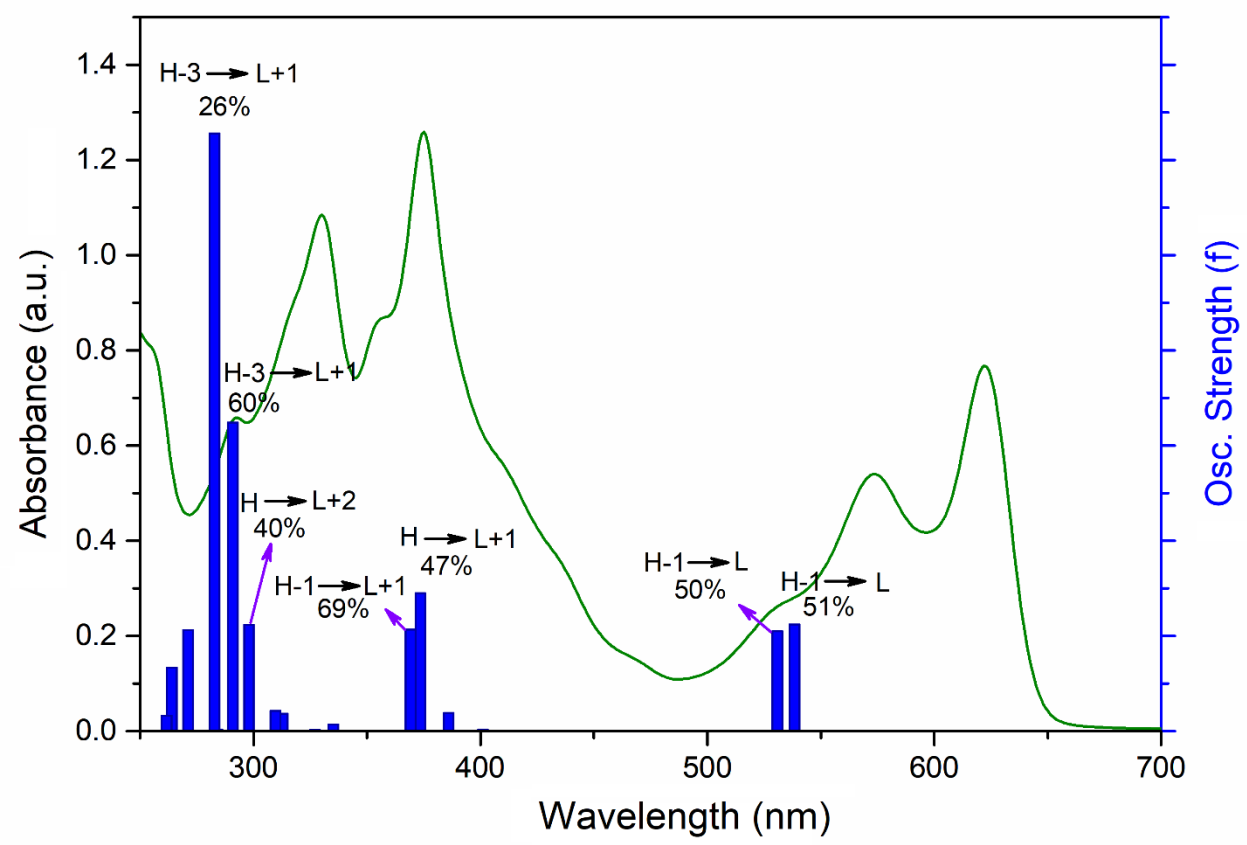

Figure S7.2. Calculated oscillator strength on the basis of optimized structure (bar) and observed absorption spectra (line) of **4**.

Table S7.2: Transition energies, oscillator strength and orbital contributions calculated for **4** TD-DFT analysis at (TD) B3LYP/6-31g(d) level of theory (H = HOMO, L= LUMO)

Transition	Wavelength (nm)	Oscillator Strength (f)	Major Contributors
$S_0 \rightarrow S_1$	538.33	0.2242	H → L (51.44%) H-1 → L (34.16%)
$S_0 \rightarrow S_2$	530.88	0.2101	H-1 → L (50.11%) H → L (33.68%)
$S_0 \rightarrow S_3$	474.00	0.0003	H-2 → L (97.37%)
$S_0 \rightarrow S_4$	401.08	0.0039	H-3 → L (86.84%)
$S_0 \rightarrow S_5$	385.95	0.0386	H-4 → L (93.39%)
$S_0 \rightarrow S_6$	373.47	0.2903	H → L+1 (47.16%) H-5 → L (38.92%)
$S_0 \rightarrow S_7$	369.14	0.2135	H-1 → L+1 (69.01%)
$S_0 \rightarrow S_8$	335.31	0.0006	H-8 → L (96.15%)
$S_0 \rightarrow S_9$	335.07	0.0142	H-2 → L+1 (86.15%)
$S_0 \rightarrow S_{10}$	331.35	0.0000	H-9 → L (95.52%)
$S_0 \rightarrow S_{11}$	327.05	0.0025	H-6 → L (54.88%) H → L+2 (43.46%)
$S_0 \rightarrow S_{12}$	312.77	0.0372	H-7 → L (50.37%) H-1 → L+2 (28.29%)
$S_0 \rightarrow S_{13}$	309.64	0.0423	H-1 → L+2 (46.44%) H-7 → L (39.55%)
$S_0 \rightarrow S_{14}$	297.93	0.2233	H-3 → L+1 (59.56%) H-5 → L (16.76%)
$S_0 \rightarrow S_{15}$	290.85	0.6485	H-3 → L+1 (59.56%) H-5 → L (16.76%)
$S_0 \rightarrow S_{16}$	283.93	0.0034	H-4 → L+1 (88.65%)
$S_0 \rightarrow S_{17}$	282.69	1.2563	H-3 → L+1 (26.23%) H-5 → L (21.64%)
$S_0 \rightarrow S_{18}$	271.17	0.2124	H-2 → L+2 (56.24%) H-1 → L+3 (24.02%)
$S_0 \rightarrow S_{19}$	263.97	0.1333	H → L+3 (65.30%)
$S_0 \rightarrow S_{20}$	261.67	0.0325	H-5 → L+1 (57.58%)

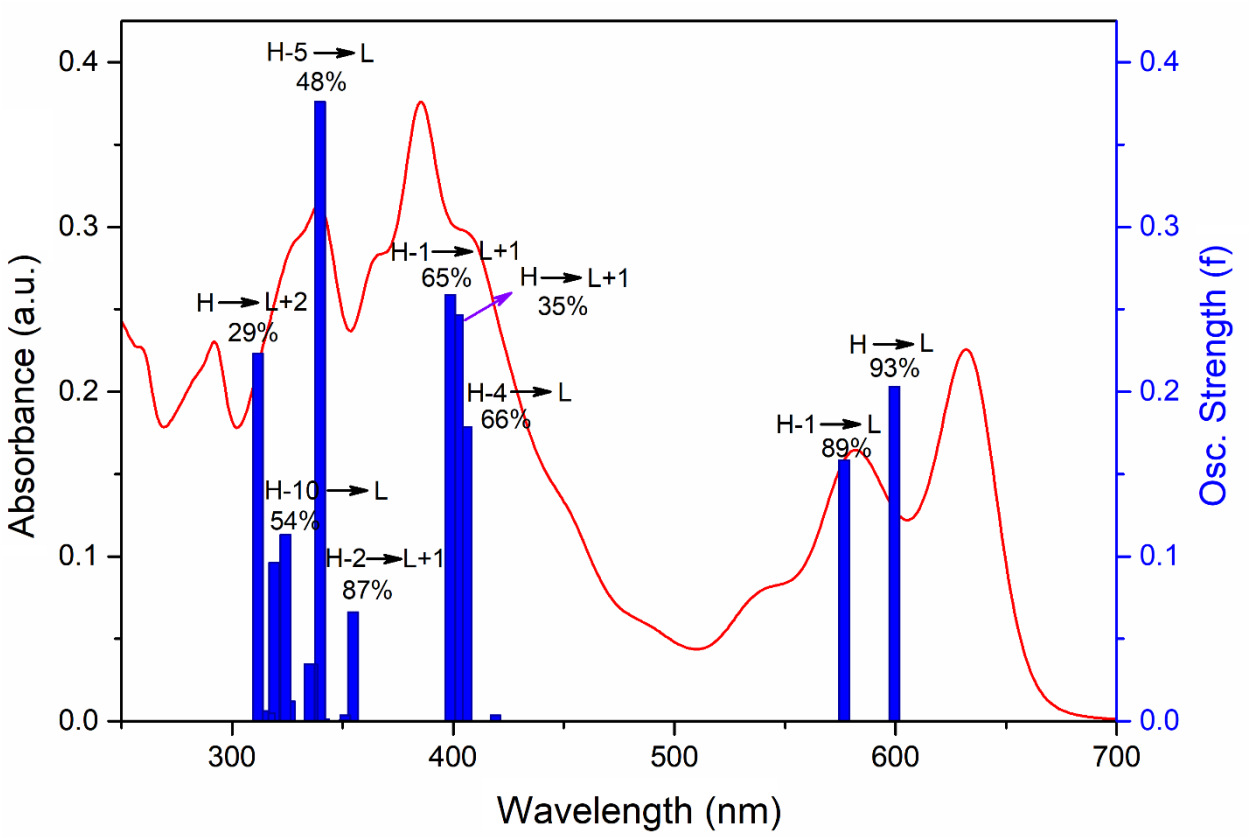

Figure S7.3. Calculated oscillator strength on the basis of optimized structure (bar) and observed absorption spectra (line) of **5**.

Table S7.3: Transition energies, oscillator strength and orbital contributions calculated for **5** from TDDFT analysis at (TD)B3LYP/6-31g(d) level of theory (H = HOMO, L= LUMO)

Transition	Wavelength (nm)	Oscillator Strength (f)	Major Contributors
$S_0 \rightarrow S_1$	599.39	0.2032	H → L (92.66%)
$S_0 \rightarrow S_2$	576.74	0.1585	H-1 → L (89.08%)
$S_0 \rightarrow S_3$	501.05	0.0003	H-2 → L (98.04%)
$S_0 \rightarrow S_4$	419.07	0.0035	H-3 → L (86.60%)
$S_0 \rightarrow S_5$	405.98	0.1785	H-4 → L (66.50%) H → L+1(26.44%)
$S_0 \rightarrow S_6$	401.91	0.2466	H → L+1(35.55%) H-4 → L (25.30%)

$S_0 \rightarrow S_7$	398.60	0.2588	H-1 → L+1 (64.99%)
$S_0 \rightarrow S_8$	354.73	0.0662	H-2 → L+1 (87.27%)
$S_0 \rightarrow S_9$	351.21	0.0037	H-6 → L (97.78%)
$S_0 \rightarrow S_{10}$	350.90	0.0007	H-7 → L (97.80%)
$S_0 \rightarrow S_{11}$	341.54	0.0012	H-12 → L (85.23%)
$S_0 \rightarrow S_{12}$	339.77	0.3760	H-5 → L (47.56%)
$S_0 \rightarrow S_{13}$	336.20	0.0346	H-13 → L (88.00%)
$S_0 \rightarrow S_{14}$	335.01	0.0346	H-8 → L (74.77%)
$S_0 \rightarrow S_{15}$	326.12	0.0120	H-9 → L (80.16%)
$S_0 \rightarrow S_{16}$	324.14	0.1131	H-10 → L (54.19%) H-11 → L (32.79%)
$S_0 \rightarrow S_{17}$	318.94	0.0961	H → L+3 (31.87%) H-1 → L+2 (28.18%)
$S_0 \rightarrow S_{18}$	317.09	0.0048	H-1 → L+2 (41.73%)
$S_0 \rightarrow S_{19}$	314.17	0.0063	H → L+4 (71.08%)
$S_0 \rightarrow S_{20}$	311.73	0.2232	H → L+2 (28.48%)

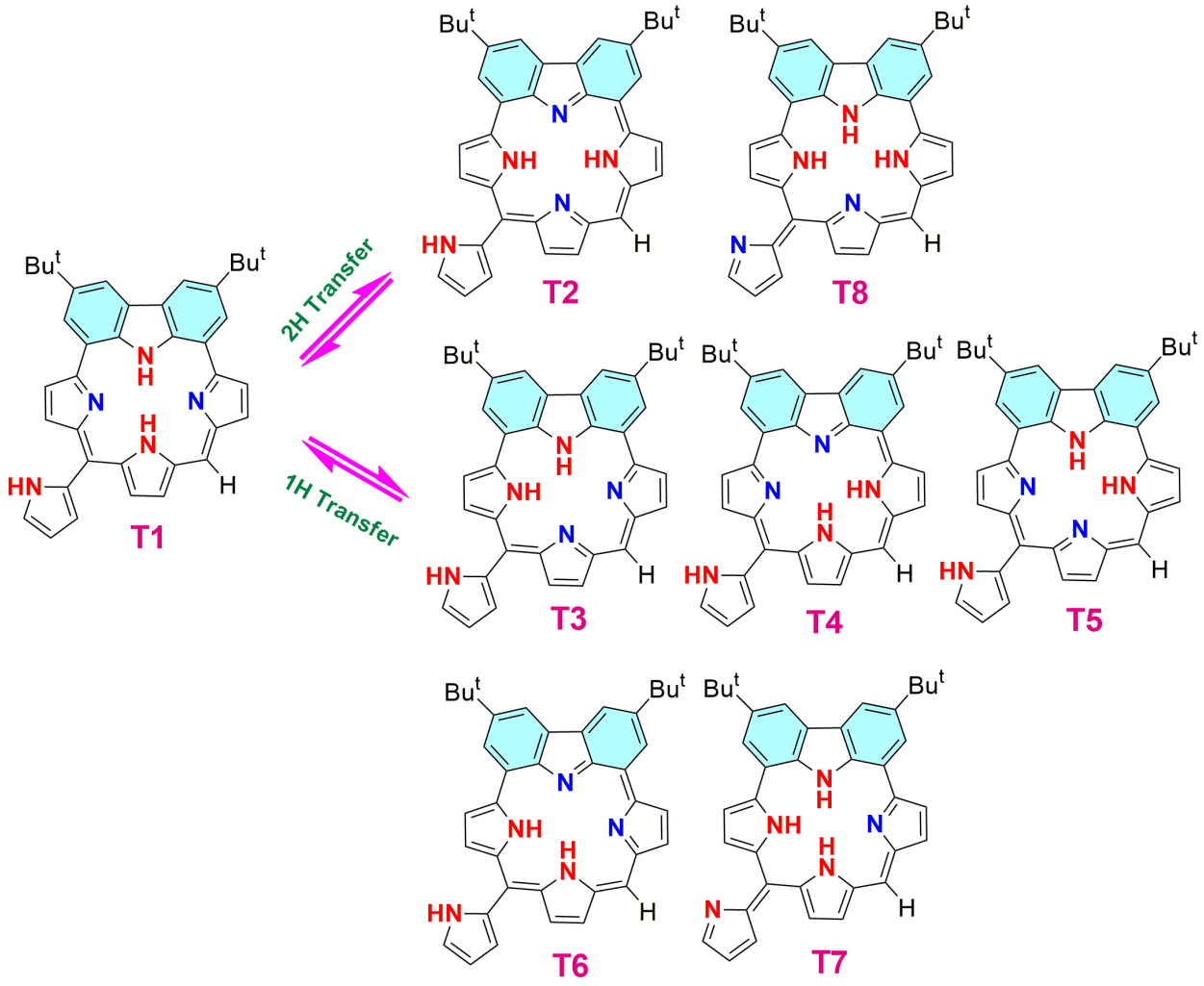

Table S7.4: Relative free energies of various tautomers (T1-T8) of **3**, calculated at the B3LYP/6-31g(d) level of theory. The solvent effect was accounted for using the polarizable continuum model (PCM).

Tautomers	**T1**	**T2**	**T3**	**T4**	**T5**	**T6**	**T7**	**T8**
Rel. energy (kcal mol^{-1})	0	+2.22	+7.12	+9.35	+11.24	+12.58	+13.59	+18.69

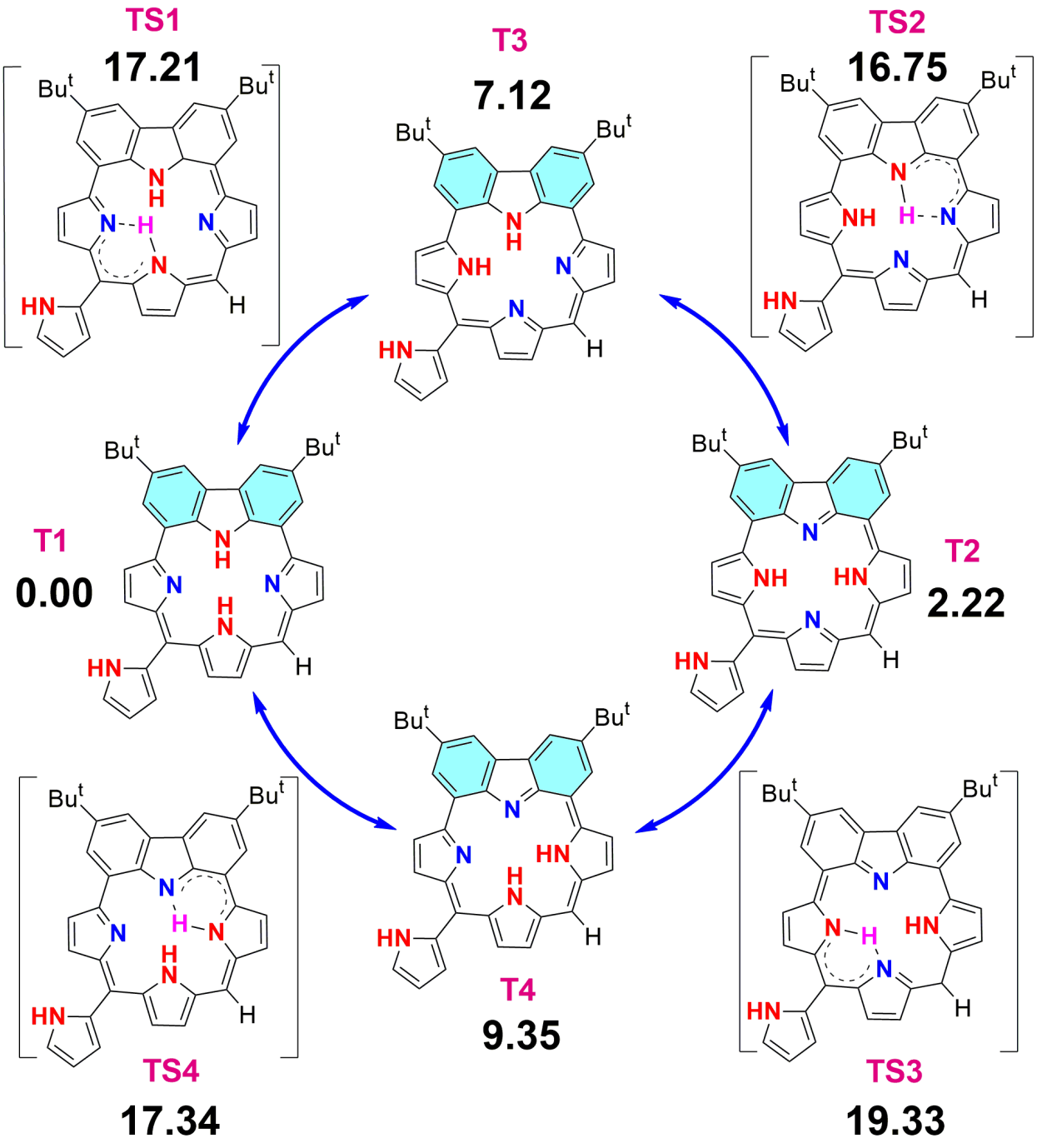

Figure S7.3. Various *cis*-tautomers for interconversion of **T1↔T2** along with their transition-states. All the energies are given in kcal mol^{-1}.

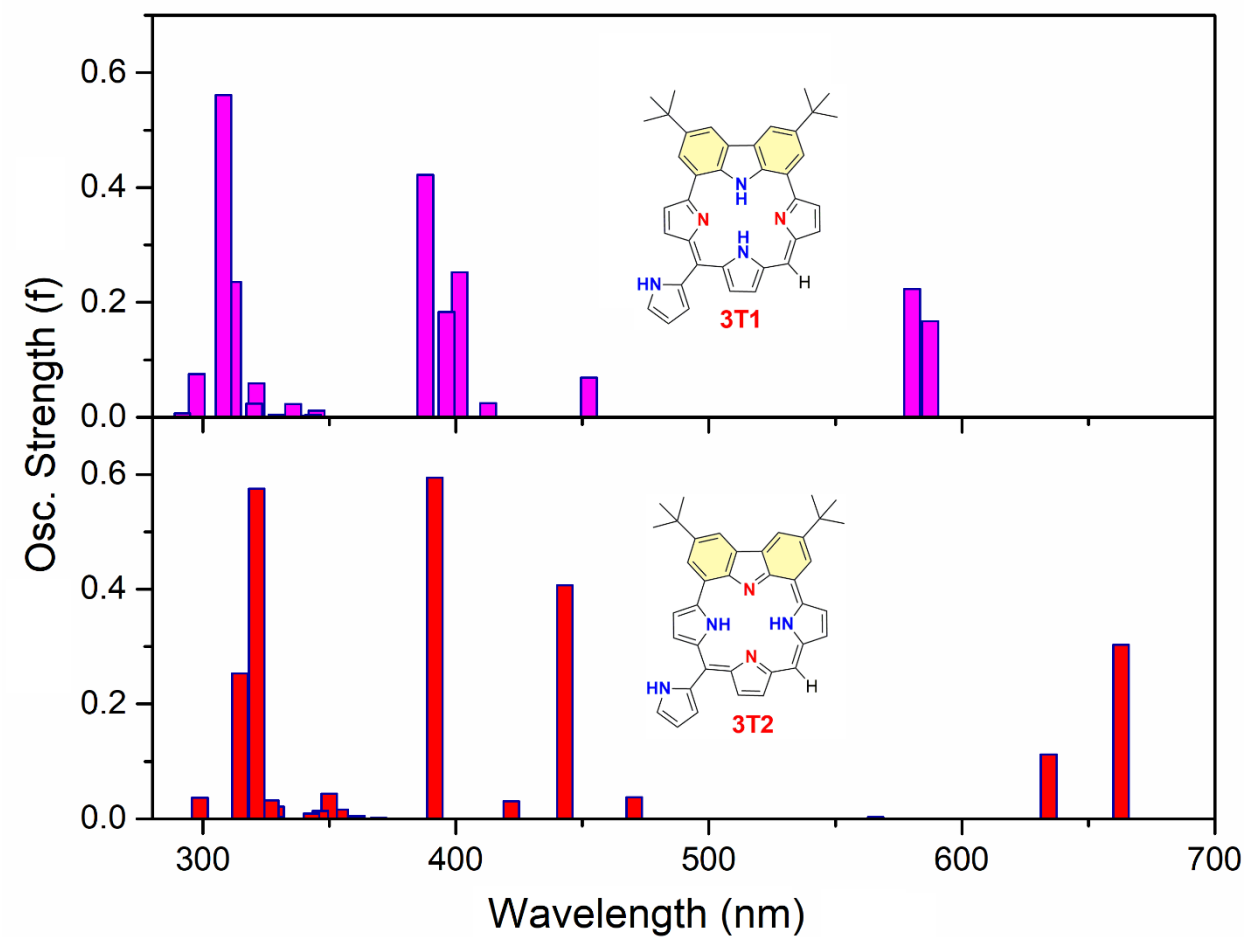

Figure S7.4. Simulated electronic absorption spectra of **3T1** (top) and **3T2** (bottom).

8. NICS Calculations

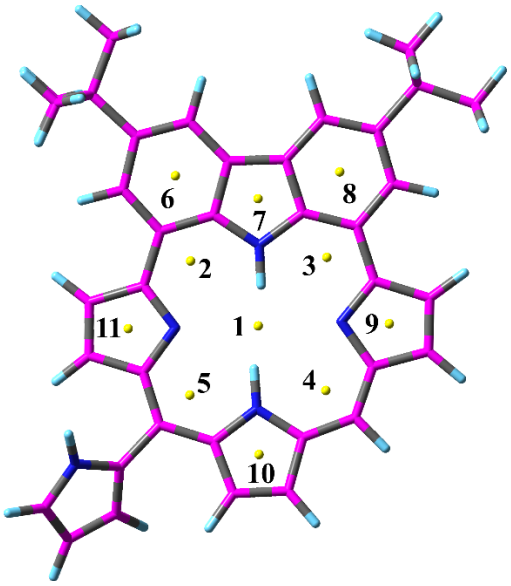

Position	NICS (ppm)	Position	NICS (ppm)
1	**-2.84**	**7**	-5.25
2	-5.36	**8**	-11.49
3	-5.09	**9**	-2.70
4	-6.81	**10**	-11.17
5	-5.62	**11**	-3.34
6	-11.51		

Figure S8.1. NICS(0) values at various positions of **3**.

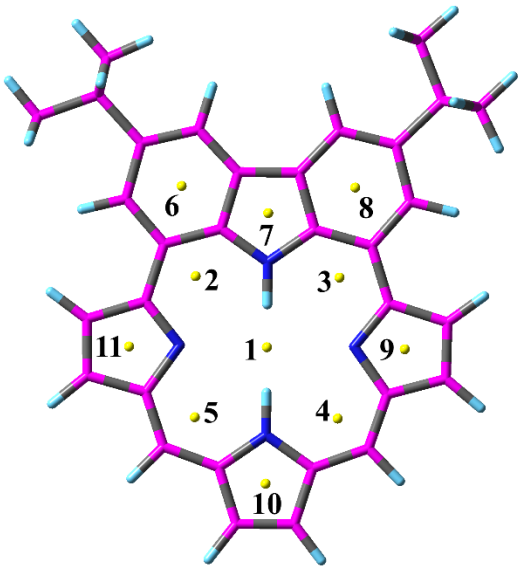

Position	NICS (ppm)	Position	NICS (ppm)
1	**-3.29**	**7**	-4.98
2	-5.72	**8**	-11.71
3	-5.67	**9**	-2.78
4	-6.98	**10**	-11.50
5	-7.00	**11**	-2.66
6	-11.59		

Figure S8.2. NICS(0) values at various positions of **4**.

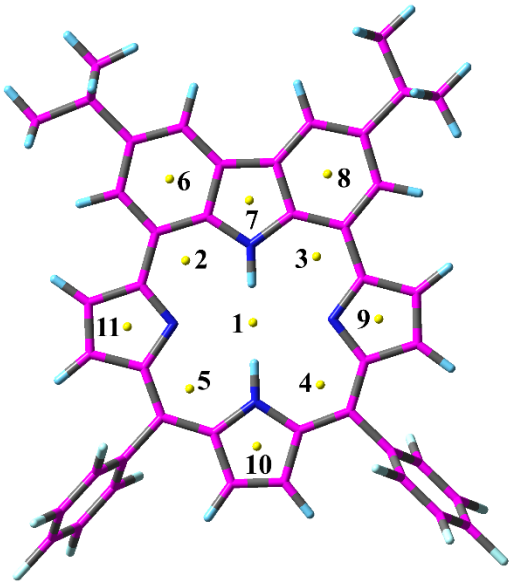

Position	NICS (ppm)	Position	NICS (ppm)
1	**-3.58**	**7**	-4.69
2	-6.22	**8**	-11.77
3	-6.17	**9**	-2.00
4	-6.58	**10**	-11.28
5	-6.61	**11**	-1.87
6	-11.61		

Figure S8.3. NICS(0) values at various positions of **5**.

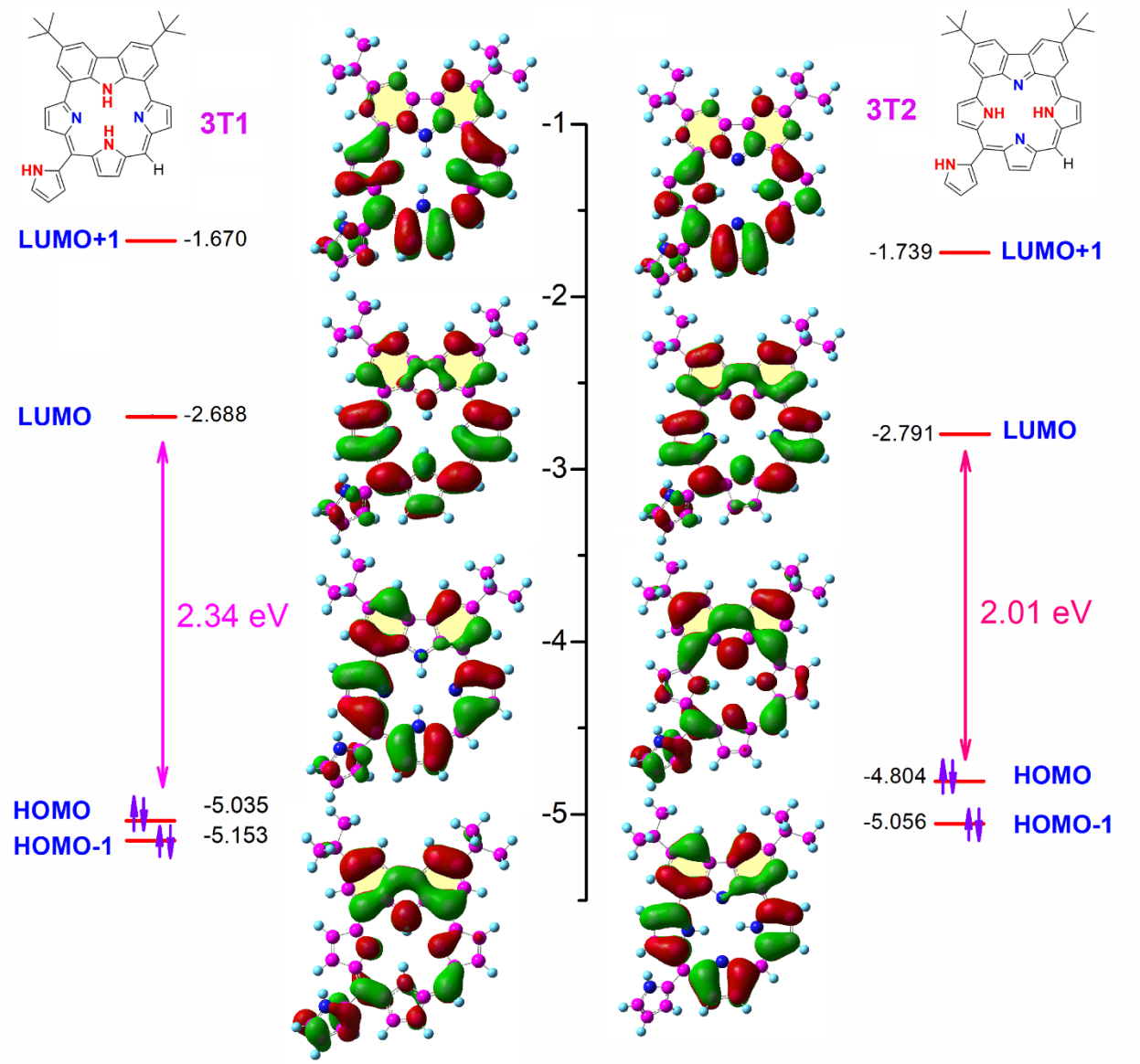

Figure S8.5. Energy level diagrams of **3T1** and **3T2** calculated at the B3LYP/6-31g(d) level.

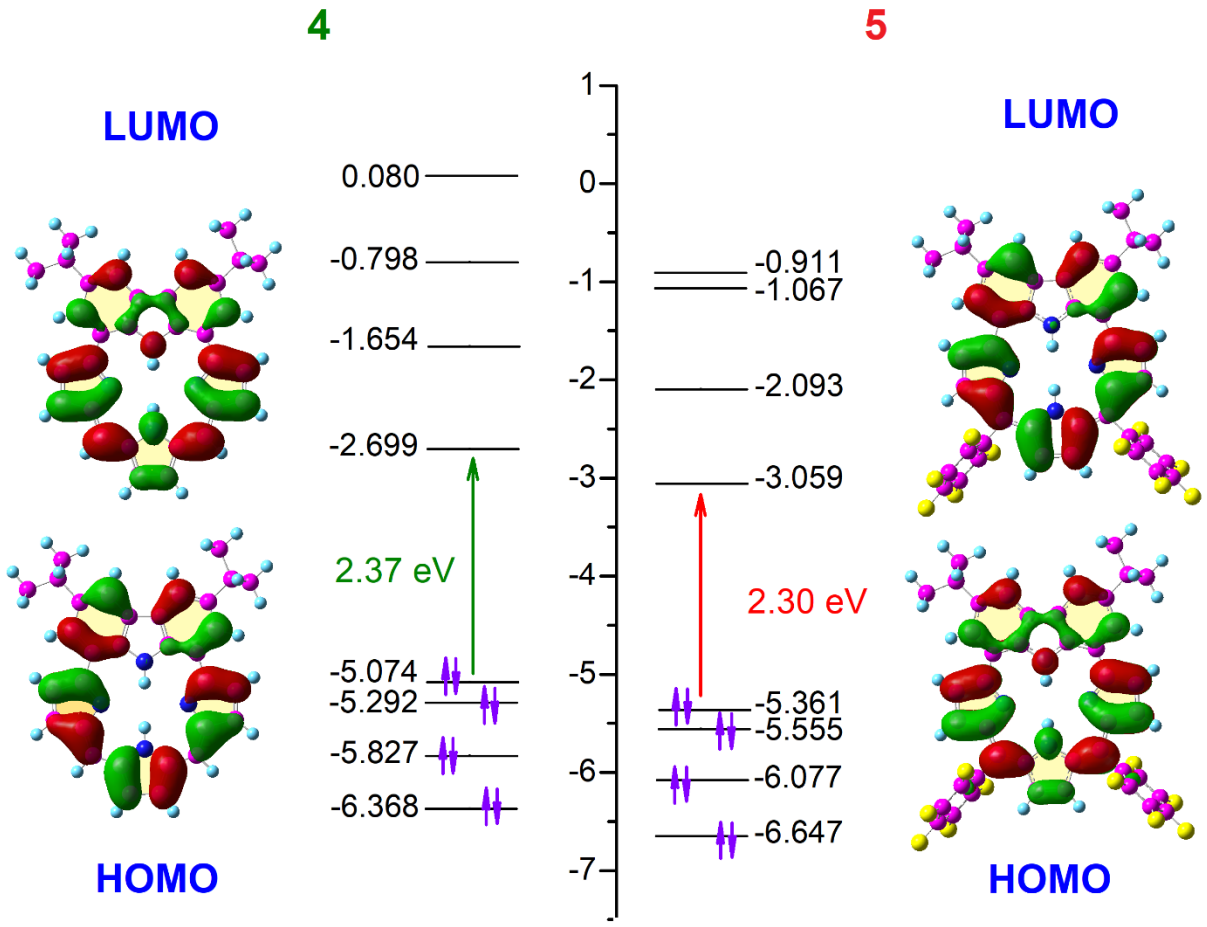

Figure S8.6. Energy level diagrams of **4** and **5** calculated at the B3LYP/6-31g(d) level.

9. Cyclic voltammetry

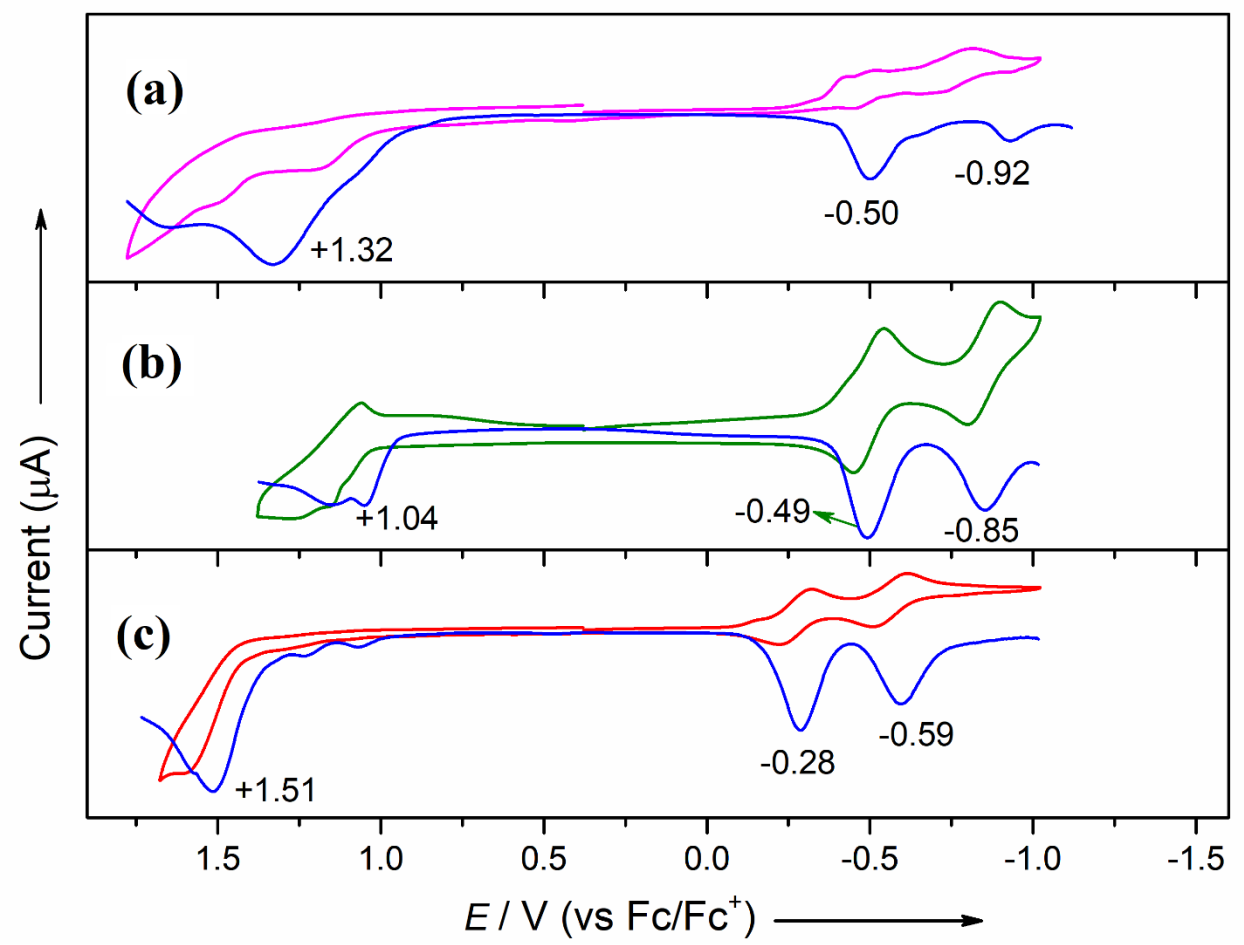

Figure S9.1. Cyclic Voltammetry and DPV for (a) **3** (b) **4** and (c) **5** recorded in CH_2Cl_2.

Table S9.1. Summary of the redox potentials.[a]

Macrocycles	$E^{1/2}_{ox.1}$/V	$E^{1/2}_{red.1}$/V	$E^{1/2}_{red.2}$/V	ΔE_{cv}/eV	ΔE_{opt}/eV	ΔE_{DFT}/eV
3	1.32[b]	-0.50	-0.92	1.82	1.98	2.34
4	1.04[b]	-0.49[b]	-0.85	1.53	2.00	2.37
5	1.51[b]	-0.28	-0.59[b]	1.79	1.97	2.30

[a]Potentials[V] vs ferrocene/ferrocenium ion. Scan rate 0.05 Vs^{-1}; working electrode, glassy carbon; counter electrode, Pt wire; supporting electrolyte, 0.1 M $^{n}Bu_4NPF_6$; reference electrode, saturated calomel electrode. [b]Determined by differential pulse voltammetry.

10. Decay profiles and AICD plots

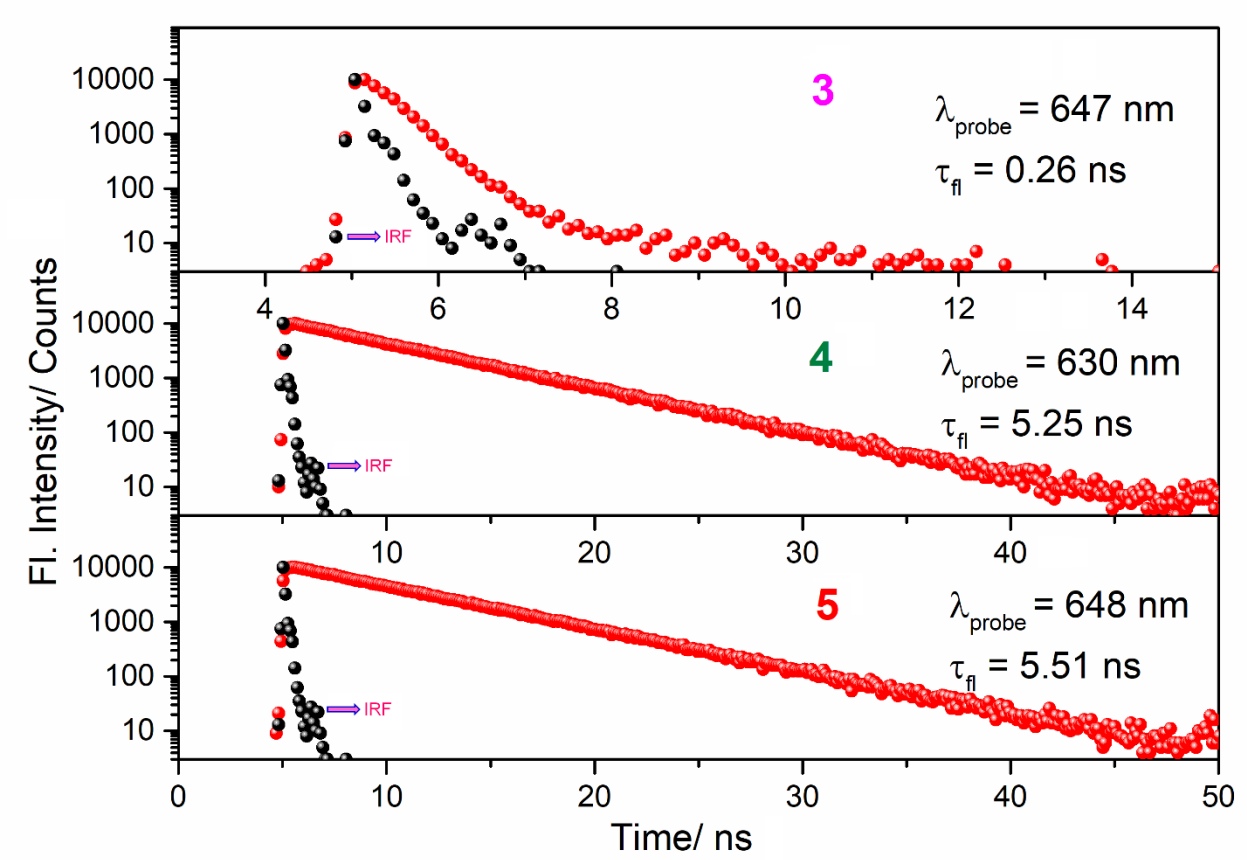

Figure S10.1. Time-correlated single photon counting (TCSPC) of **3** (*meso*-pyrrole), **4** (bis *meso*-free) and **5** (bis-*meso*-C_6F_5) recorded in toluene at 298 K. λ_{ex} = 440 nm.

Table S10.1: Photophysical data of **3-5**

macrocycles	λ_{ex}	Φ_F[a] (%)	τ_F (ns)	k_r[b] (10^8 s^{-1})	k_{nr}[b] (10^8 s^{-1})
3	600	7.21	0.26	2.773	35.68
	440	3.30	0.26	1.269	37.19
4	600	30.93	5.25	0.589	1.315
5	600	26.10	5.51	0.473	1.341

[a]Using **NH-carbz**[S9] as reference (λ_{ex} = 440 and 600 nm, Φ_F = 28.9% in toluene).
[b]$k_r = \Phi_F/\tau_F$, $k_{nr} = (1-\Phi_F)/\tau_F$, assuming that the emitting state is produced with unit quantum efficiency.

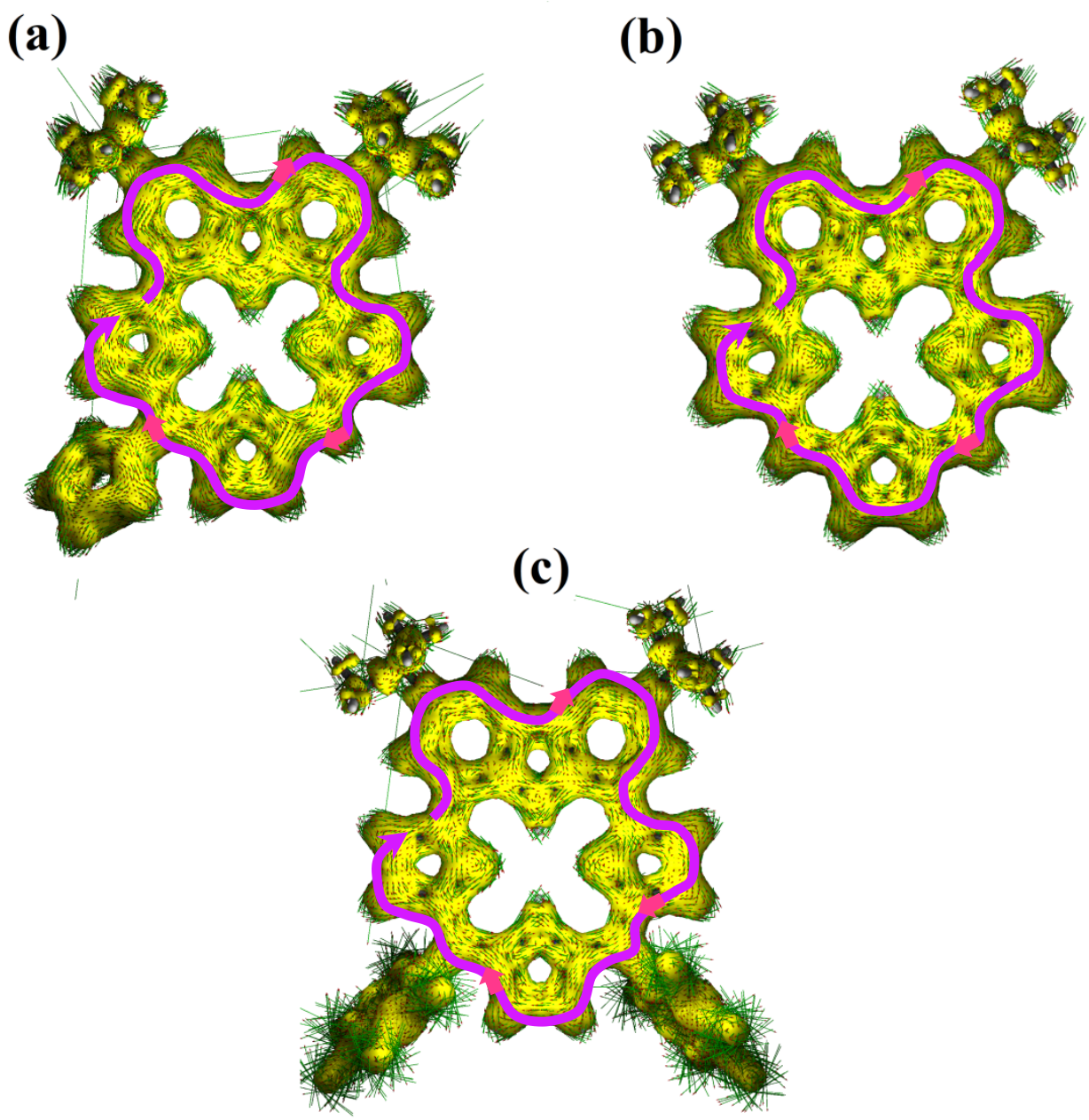

Figure S10.2. ACID plots for (a) **3** (*meso*-pyrrole) (b) **4** (*meso*-free porphyrin) and (c) **5** (Bis *meso*-C_6F_5) Vectors moving clock-wise direction is indicated by the appropriate arrows.

10. Supporting References:

[S1] Gaussian 16, Revision A.03, M. J. Frisch, G. W. Trucks, H. B. Schlegel, G. E. Scuseria, M. A. Robb, J. R. Cheeseman, G. Scalmani, V. Barone, G. A. Petersson, H. Nakatsuji, X. Li, M. Caricato, A. V. Marenich, J. Bloino, B. G. Janesko, R. Gomperts, B. Mennucci, H. P. Hratchian, J. V. Ortiz, A. F. Izmaylov, J. L. Sonnenberg, D. Williams-Young, F. Ding, F. Lipparini, F. Egidi, J. Goings, B. Peng, A. Petrone, T. Henderson, D. Ranasinghe, V. G. Zakrzewski, J. Gao, N. Rega, G. Zheng, W. Liang, M. Hada, M. Ehara, K. Toyota, R. Fukuda, J. Hasegawa, M. Ishida, T. Nakajima, Y. Honda, O. Kitao, H. Nakai, T. Vreven, K. Throssell, J. A. Montgomery, Jr., J. E. Peralta, F. Ogliaro, M. J. Bearpark, J. J. Heyd, E. N. Brothers, K. N. Kudin, V. N. Staroverov, T. A. Keith, R. Kobayashi, J. Normand, K. Raghavachari, A. P. Rendell, J. C. Burant, S. S. Iyengar, J. Tomasi, V. Cossi, J. M. Millam, V. Klene, C. Adamo, R. Cammi, J. W. Ochterski, R. L. Martin, K. Morokuma, O. Farkas, J. B. Foresman and D. J. Fox, Gaussian, Inc., Wallingford CT, 2016

[S2] a) D. Geuenich, K. Hess, V. Köhler and R. Herges, *Chem. Rev*., 2005, **105**, 3758-3772; b) R. Herges and R. Geuenich, *J. Phys. Chem. A,* 2001, **105**, 3214-3220; c) R. Herges, *Chem. Rev.,* 2006, **106**, 4820-4842. d) R. A. Vogt, G. T. Gray, C. E. Crespo-Hernández, *J. Am. Chem. Soc*., 2012, S14.

[S3] G. M. Peters, J. B. Winegrad, M. R. Gau, G. H. Imler, B. Xu, S. Ren, B. B. Wayland and M. J. Zdilla, *Inorg. Chem*. 2017, **56**, 3377-3385.

[S4] H. Mori, K. Naoda and A. Osuka, *Asian J. Org. Chem*. 2013, **2**, 600-605.

[S5] P. D. Rao, B. J. Littler, G. R. Geier and J. S. Lindsey, *J. Org. Chem*. 2000, **65**, 1084-1092.